Renewable and Sustainable Energy Reviews 202 (2024) 114674

Contents lists available at ScienceDirect

Renewable and Sustainable Energy Reviews

journal homepage: www.elsevier.com/locate/rser

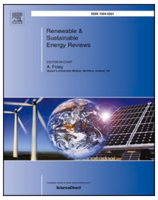

Energy and economic assessment of hydrothermal-treatment-coupled anaerobic digestion

Chiqian Zhang[a,*], Kainat Rahnuma[a], Liyuan Hou[b,c], Xiaoguang Liu[d], Yuanzhi Tang[e], Spyros G. Pavlostathis[f]

[a] Civil Engineering Program, College of Engineering & Computer Science, Arkansas State University, Jonesboro, AR 72467, USA
[b] Department of Civil and Environmental Engineering, Utah State University, Logan, UT 84322, USA
[c] Utah Water Research Laboratory, Logan, UT 84321, USA
[d] State Key Laboratory of Pollution Control and Resources Reuse, College of Environmental Science and Engineering, Tongji University, Shanghai 200092, China
[e] School of Earth and Atmospheric Sciences, Georgia Institute of Technology, Atlanta, GA 30332, USA
[f] School of Civil and Environmental Engineering, Georgia Institute of Technology, Atlanta, GA 30332, USA

ARTICLE INFO

Keywords:
Municipal wastewater
Sewage sludge
Anaerobic digestion
Hydrothermal treatment
Energy balance
Economic assessment
Electricity
Heat
Biogas
Biomethane
Carbon dioxide
Renewable energy

ABSTRACT

Hydrothermal treatment enhances biomethane (renewable energy source) production from the anaerobic digestion of municipal sewage sludge but requires substantial energy (heat). A complete energy and economic analysis for a hydrothermal-treatment-coupled anaerobic digestion system is missing. This study comprehensively analyzes the energy and economic aspects of three hydrothermal-treatment-coupled anaerobic digestion systems plus a control for municipal sludge treatment: A control (anaerobic digestion only), a pre-stage system, an inter-stage system, and a post-stage/recycle system. The large energy consumption of hydrothermal treatment challenges the overall energy and economic neutrality in the systems. Hydrothermal treatment is economically beneficial only if it is conducted at a low or moderate temperature (100 to 130 °C), when the raw sludge has a high content of complex organic matter (especially particulate organic matter), and when the control has a low biogas yield. To reduce the energy burden of hydrothermal treatment and make the systems more economically beneficial, this study proposes to use direct sunlight as a “free,” renewable energy source to conduct hydrothermal treatment. In addition, the energy consumption of hydrothermal treatment can be reduced by separating the solids and liquid fractions in sludge using centrifugation and applying hydrothermal treatment to only the solids. Recovering carbon dioxide from the biogas has significant environmental and economic benefits. Among the alternatives, the post-stage/recycle system is more beneficial from an economic viewpoint and should be considered in future studies. Conversely, the inter-stage system should be avoided because it is more complex to maintain, requires a larger footprint, and has less significant economic benefits.

Nomenclature

AB	Anaerobic bioreactor
AD	Anaerobic digestion
CHP	Combined heat and power
COD	Chemical oxygen demand
HT	Hydrothermal treatment
PS	Primary sludge
SRT	Solids retention time
TS	Total solids
VS	Volatile solids
WAS	Waste activated sludge
WRRFs	Water resource recovery facilities

Notations/Symbols and Units

Notation	Explanation	Unit
$A_{f/c\text{-}AD}$	Surface area of the floor or cover of an AB	m^2
$A_{f\text{-}HT}$	Floor area of an HT device	m^2
A_{HT}	Total surface area of an HT device	m^2
$A_{w\text{-}AD}$	Surface area of the wall of an AB	m^2
C_c	Constant-pressure specific heat capacity of carbon dioxide at 308.15 K	$kJ \cdot kg^{-1}_{\text{Carbon dioxide}} \cdot K^{-1}$

(*continued on next page*)

---

* Corresponding author.
E-mail address: czhang@astate.edu (C. Zhang).

https://doi.org/10.1016/j.rser.2024.114674
Received 20 December 2023; Received in revised form 7 May 2024; Accepted 14 June 2024

1364-0321/© 2024 Elsevier Ltd. All rights are reserved, including those for text and data mining, AI training, and similar technologies.

(*continued*)

Notation	Explanation	Unit
$C_{k,\ s,\ AD\text{-}j}$	Specific heat capacity of the digestate from AB *j* in the k^{th} system	$\text{kJ}\cdot\text{kg}^{-1}_{\text{Sludge}}\cdot\text{K}^{-1}$
$C_{k,\ s,\ AD\text{-}j,\ in}$	Specific heat capacity of the influent of AB *j* in the k^{th} system	$\text{kJ}\cdot\text{kg}^{-1}_{\text{Sludge}}\cdot\text{K}^{-1}$
$C_{k,\ s,\ HT}$	Specific heat capacity of the influent and effluent of the HT device in the k^{th} system	$\text{kJ}\cdot\text{kg}^{-1}_{\text{Sludge}}\cdot\text{K}^{-1}$
C_m	Constant-pressure specific heat capacity of methane at 308.15 K	$\text{kJ}\cdot\text{kg}^{-1}_{\text{Methane}}\cdot\text{K}^{-1}$
C_{wv}	Constant-pressure specific heat capacity of water vapor at 308.15 K	$\text{kJ}\cdot\text{kg}^{-1}_{\text{Water vapor}}\cdot\text{K}^{-1}$
$d_{c\text{-}AD}$	Thickness of the cover of an AB	cm
$d_{f/w\text{-}AD}$	Thickness of the floor or wall of an AB	cm
d_{HT}	Thickness of the floor, wall, or cover of an HT device	cm
D_{AD}	Diameter of an AB	m
D_{HT}	Diameter of an HT device	m
$EC_{\text{C}_{10}\text{H}_{19}\text{O}_3\text{N}}$	Energy content of dry sludge organic matter	$\text{kJ}\cdot\text{g}^{-1}$ COD or $\text{kJ}\cdot\text{mol}^{-1}$
$E_{k,\ CHP}$	Total electricity generated by the CHP unit in the k^{th} system	$\text{kJ}\cdot\text{d}^{-1}$
$E_{k,\ CHP\text{-}p/m}$	Amount of the electricity generated from the CHP unit in the k^{th} system that is used to pump and mix sludge	$\text{kJ}\cdot\text{d}^{-1}$
$E_{k,\ CHP\text{-}sep}$	Amount of the electricity generated from the CHP unit in the k^{th} system that is used to separate carbon dioxide and biomethane in the biogas and to liquefy carbon dioxide	$\text{kJ}\cdot\text{d}^{-1}$
$E_{k,\ CHP\text{-}re}$	The rest of the electricity generated from the CHP unit in the k^{th} system (after pumping and mixing sludge, separating carbon dioxide from the biogas, and liquefying carbon dioxide)	$\text{kJ}\cdot\text{d}^{-1}$
$E_{k,\ p/m}$	Total electricity demand for pumping and mixing sludge in the k^{th} system	$\text{kJ}\cdot\text{d}^{-1}$
$E_{k,\ tot}$	Overall economic aspects of the k^{th} system	$\$\cdot\text{d}^{-1}$
$E_{m\text{-}AD}$	Electricity required to mix sludge in an AB	$\text{kJ}\cdot\text{d}^{-1}$
$E_{m\text{-}HT}$	Electricity required to mix sludge in an HT device	$\text{kJ}\cdot\text{d}^{-1}$
$E_{p\text{-}AD}$	Electricity required to pump sludge into an AB	$\text{kJ}\cdot\text{d}^{-1}$
$E_{p\text{-}HT}$	Electricity required to pump sludge into an HT device	$\text{kJ}\cdot\text{d}^{-1}$
f_c	The percentage of the electrons provided by the electron donor that is used for biomass synthesis during AD	%
f_{cd}	Volumetric ratio of carbon dioxide in the biogas	%
f_e	The percentage of the electrons provided by the electron donor that is used for energy production during AD	%
f_m	Volumetric ratio of biomethane in the biogas	%
f_{VS}	Mass ratio of VS to TS in municipal sludge	%
F	Volumetric flow rate of municipal sewage sludge in the WRRF	$\text{m}^3_{\text{Sludge}}\cdot\text{d}^{-1}$
h_a	Conductive heat transfer coefficient between still air and stainless steel	$\text{W}\cdot\text{m}^{-2}\cdot\text{K}^{-1}$
h_{sl}	Conductive heat transfer coefficient between sludge and stainless steel	$\text{W}\cdot\text{m}^{-2}\cdot\text{K}^{-1}$
H_{HT}	Height of an HT device	m
$H_{mi\text{-}AD}$	Middle height of an AB	m
$H_{si\text{-}AD}$	Side height of an AB	m
I	Annual average solar radiation incident on an AB or an HT device	$\text{kJ}\cdot\text{m}^{-2}\cdot\text{d}^{-1}$
MM_c	Molar mass of carbon dioxide	$\text{kg}\cdot\text{mol}^{-1}$
MM_m	Molar mass of methane	$\text{kg}\cdot\text{mol}^{-1}$
MM_w	Molar mass of water	$\text{kg}\cdot\text{mol}^{-1}$
MV	Molar volume of an ideal gas at 35 °C and 1 atm	$\text{m}^3_{\text{Gas}}\cdot\text{mol}^{-1}$
$P_{c\text{-}s}$	Wholesale market price of food-grade liquid carbon dioxide in the United States	$\$\cdot\text{kg}^{-1}$
$P_{e\text{-}s}$	Wholesale market price of the surplus electricity generated from the CHP unit	$\$\cdot\text{kJ}^{-1}$
$P_{e\text{-}p}$	Ultimate consumer electricity price for the industrial sector in the United States	$\$\cdot\text{kJ}^{-1}$
$P_{h\text{-}s}$	Wholesale market price of the surplus heat generated from the CHP unit	$\$\cdot\text{kJ}^{-1}$
P_{wv}	Saturation pressure of water vapor in the biogas	Pa
$Q_{em\text{-}AD}$	The net radiant energy emission from an AB	$\text{kJ}\cdot\text{d}^{-1}$
$Q_{em\text{-}HT}$	The net radiant energy emission from an HT device	$\text{kJ}\cdot\text{d}^{-1}$
$Q_{k,\ CHP}$	Total heat generated by the CHP unit in the k^{th} system	$\text{kJ}\cdot\text{d}^{-1}$
$Q_{k,\ de\text{-}AD}$	Overall heat demand of the AB(s) in the k^{th} system	$\text{kJ}\cdot\text{d}^{-1}$
$Q_{k,\ de\text{-}HT}$	Overall heat demand of the HT device in the k^{th} system	$\text{kJ}\cdot\text{d}^{-1}$
$Q_{k,\ esc\text{-}AD\text{-}j}$	Heat loss from AB *j* due to the escape of carbon dioxide in the biogas in the k^{th} system	$\text{kJ}\cdot\text{d}^{-1}$
$Q_{k,\ esm\text{-}AD\text{-}j}$	Heat loss from AB *j* due to the escape of biomethane in the biogas in the k^{th} system	$\text{kJ}\cdot\text{d}^{-1}$
$Q_{k,\ evw\text{-}AD\text{-}j}$	Heat loss from AB *j* due to the escape of water vapor in the biogas in the k^{th} system	$\text{kJ}\cdot\text{d}^{-1}$
$Q_{k,\ ex\text{-}AD\text{-}j}$	Heat recovered by a heat exchanger from the digestate of AB *j* in the k^{th} system that is used to heat the sludge	$\text{kJ}\cdot\text{d}^{-1}$
$Q_{k,\ ex\text{-}HT}$	Heat recovered by a heat exchanger from the effluent of the HT device in the k^{th} system	$\text{kJ}\cdot\text{d}^{-1}$
$Q_{k,\ exs\text{-}CHP}$	Heat recovered by heat exchangers from the CHP unit in the k^{th} system	$\text{kJ}\cdot\text{d}^{-1}$
$Q_{k,\ li\text{-}j}$	Heat released due to anaerobic fermentation within AB *j* in the k^{th} system at 308.15 K	$\text{kJ}\cdot\text{d}^{-1}$
$Q_{k,\ r\text{-}AD\text{-}j}$	Heat required to raise the sludge temperature to the mesophilic AD temperature for AB *j* in the k^{th} system	$\text{kJ}\cdot\text{d}^{-1}$
$Q_{k,\ r\text{-}HT}$	Heat required to raise the sludge temperature to the target HT temperature in the k^{th} system	$\text{kJ}\cdot\text{d}^{-1}$
$Q_{so\text{-}AD}$	Heat gained from solar radiation through the cover and wall of an AB	$\text{kJ}\cdot\text{d}^{-1}$
$Q_{so\text{-}HT}$	Heat gained from solar radiation through the cover and wall of an HT device	$\text{kJ}\cdot\text{d}^{-1}$
$Q_{su\text{-}AD}$	Heat loss from an AB due to the temperature difference between the surface and the surroundings	$\text{kJ}\cdot\text{d}^{-1}$
$Q_{su\text{-}HT}$	Heat loss from an HT device due to the temperature difference between the surface and the surroundings	$\text{kJ}\cdot\text{d}^{-1}$
R	Universal gas constant	$\text{kJ}\cdot\text{mol}^{-1}\cdot\text{K}^{-1}$
t_{HT}	Average retention time of sludge in an HT device	h
T	Assumed temperature of the standard state condition	K
T_a	Ambient air temperature	K
T_{AD}	Mesophilic temperature of AD	K
T_{HT}	Target HT temperature	K

(*continued on next page*)

(*continued*)

Notation	Explanation	Unit
$T_{k,\ s,\ AD\text{-}j,\ in}$	Temperature of the influent of AB *j* before the heat exchanger in the k^{th} system	K
$T_{k,\ s,\ HT,\ in}$	Temperature of the influent of the HT device before the heat exchanger in the k^{th} system	K
$TS_{k,\ AD\text{-}j}$	TS mass concentration of the digestate of AB *j* in the k^{th} system	%
$TS_{k,\ AD\text{-}j,\ in}$	TS mass concentration of the influent of AB *j* in the k^{th} system	%
T_{sl}	Temperature of raw municipal sewage sludge	K
T_{so}	Ambient soil temperature	K
TS_R	TS mass concentration of the raw sewage sludge	%
$U_{c\text{-}AD}$	Overall heat transfer coefficient of the cover of an AB	$\mathrm{W\cdot m^{-2}\cdot K^{-1}}$
$U_{f\text{-}AD}$	Overall heat transfer coefficient of the floor of an AB	$\mathrm{W\cdot m^{-2}\cdot K^{-1}}$
U_{HT}	Overall heat transfer coefficient of the construction material of an HT device	$\mathrm{W\cdot m^{-2}\cdot K^{-1}}$
$U_{w\text{-}AD}$	Overall heat transfer coefficient of the wall of an AB	$\mathrm{W\cdot m^{-2}\cdot K^{-1}}$
V_{AD}	Total volume of an AB	$\mathrm{m^3}$
$V_{e\text{-}AD}$	Effective working volume of an AB	$\mathrm{m^3}$
$V_{e\text{-}HT}$	Effective working volume of an HT device	$\mathrm{m^3}$
V_{HT}	Total volume of an HT device	$\mathrm{m^3}$
$V_{k,\ e\text{-}AD}$	Total effective working volume of the AB(s) in the k^{th} system	$\mathrm{m^{3}_{Reactor}}$
x_{wv}	Molar fraction of water vapor in the biogas	Dimensionless
Y_k	Overall biomethane production rate of the k^{th} system at 35 °C and 1 atm	$\mathrm{m^3_{Methane}\cdot m^{-3}_{Reactor}\cdot d^{-1}}$
$Y_{k,\ j}$	Biomethane production rate of AB *j* in the k^{th} system at 35 °C and 1 atm	$\mathrm{m^3_{Methane}\cdot m^{-3}_{Reactor}\cdot d^{-1}}$
Y_{VS}	VS-to-methane conversion factor	$\mathrm{mol_{Methane}\cdot kg^{-1}\ VS_{Destructed}}$
α_{AD}	Absorptivity of the construction material of an AB	Dimensionless
α_{HT}	Absorptivity of the construction material of an HT device	Dimensionless
β	Overall electricity loss due to transmission and other factors when heating an HT device or an AB, pumping or mixing sludge, separating biomethane and carbon dioxide in the biogas, or liquefying carbon dioxide	%
δ	Percentage of the available electricity from the CHP unit that is used to maintain the temperature of the AB(s) in the k^{th} system	%
ΔE_k	Overall electricity balance of the k^{th} system	$\mathrm{kJ\cdot d^{-1}}$
$\Delta H^{\circ}_{\mathrm{C_5H_7O_2N\text{-}Comb}}$	Standard enthalpy change for the combustion of dry anaerobic biomass	$\mathrm{kJ\cdot mol^{-1}}$
$\Delta H^{\circ}_{\mathrm{C_{10}H_{19}O_3N\text{-}AnaFerm}}$	Standard enthalpy change for the anaerobic fermentation of dry organic matter	$\mathrm{kJ\cdot mol^{-1}}$
$\Delta H^{\circ}_{\mathrm{C_{10}H_{19}O_3N\text{-}Comb}}$	Standard enthalpy change for the combustion of dry sludge organic matter	$\mathrm{kJ\cdot mol^{-1}}$
$\Delta H^{\circ}_{f(\mathrm{C_5H_7O_2N})}$	Standard enthalpy of formation of dry anaerobic biomass	$\mathrm{kJ\cdot mol^{-1}}$
$\Delta H^{\circ}_{f(\mathrm{C_{10}H_{19}O_3N})}$	Standard enthalpy of formation of dry sludge organic matter	$\mathrm{kJ\cdot mol^{-1}}$
$\Delta H^{\circ}_{f\left(\mathrm{CH_{4(g)}}\right)}$	Standard enthalpy of formation of methane gas	$\mathrm{kJ\cdot mol^{-1}}$
$\Delta H^{\circ}_{f\left(\mathrm{CO_{2(g)}}\right)}$	Standard enthalpy of formation of carbon dioxide gas	$\mathrm{kJ\cdot mol^{-1}}$
$\Delta H^{\circ}_{f\left(\mathrm{H_2O_{(l)}}\right)}$	Standard enthalpy of formation of liquid water	$\mathrm{kJ\cdot mol^{-1}}$

(*continued on next column*)

(*continued*)

Notation	Explanation	Unit
$\Delta H^{\circ}_{f\left(\mathrm{HCO^{-}_{3(aq)}}\right)}$	Standard enthalpy of formation of bicarbonate ion	$\mathrm{kJ\cdot mol^{-1}}$
$\Delta H^{\circ}_{f\left(\mathrm{N_{2(g)}}\right)}$	Standard enthalpy of formation of nitrogen gas	$\mathrm{kJ\cdot mol^{-1}}$
$\Delta H^{\circ}_{f\left(\mathrm{NH^{+}_{4(aq)}}\right)}$	Standard enthalpy of formation of ammonium cation	$\mathrm{kJ\cdot mol^{-1}}$
$\Delta H^{\circ}_{f\left(\mathrm{O_{2(g)}}\right)}$	Standard enthalpy of formation of oxygen gas	$\mathrm{kJ\cdot mol^{-1}}$
ΔH_m	Heat liberated when one mole of biomethane is produced during anaerobic fermentation	$\mathrm{kJ\cdot mol^{-1}_{Methane}}$
ΔH_w	Enthalpy (heat) of vaporization of water at 308.15 K	$\mathrm{kJ\cdot kg^{-1}_{Water\ vapor}}$
ΔQ_k	Overall heat balance of the AB(s) in the k^{th} system	$\mathrm{kJ\cdot d^{-1}}$
ε_{AD}	Emissivity coefficient of the construction material of an AB	Dimensionless
ε_{HT}	Emissivity coefficient of the construction material of an HT device	Dimensionless
η_e	Electricity conversion efficiency of a CHP unit	%
η_h	Heat conversion efficiency of a CHP unit	%
η_{TS}	Theoretical TS destruction of an HT-coupled AD system at which its overall economic aspects are the same as the control	%
θ_{AD}	SRT of an AB	d
λ	Constant used in calculating the electricity consumption for separating biomethane and carbon dioxide in the biogas	Dimensionless
μ	Energy loss in a CHP unit when cooling the biogas to remove water vapor	%
ξ	Lower heating value of methane	$\mathrm{kJ\cdot mol^{-1}_{Methane}}$
$\rho_{k,\ s,\ AD\text{-}j}$	Mass density of the digestate of AB *j* in the k^{th} system	$\mathrm{kg_{Sludge}\cdot m^{-3}_{Sludge}}$
$\rho_{k,\ s,\ AD\text{-}j,\ in}$	Mass density of the influent of AB *j* in the k^{th} system	$\mathrm{kg_{Sludge}\cdot m^{-3}_{Sludge}}$
$\rho_{k,\ s,\ HT}$	Mass density of the influent and effluent of the HT device in the k^{th} system	$\mathrm{kg_{Sludge}\cdot m^{-3}_{Sludge}}$
ρ_{ss}	Mass density of dry sludge solids	$\mathrm{kg_{TS}\cdot m^{-3}_{TS}}$
ρ_w	Mass density of the liquid portion of the digestate from an AB	$\mathrm{kg_{Liquid}\cdot m^{-3}_{Liquid}}$
σ	Stefan-Boltzmann constant	$\mathrm{W\cdot m^{-2}\cdot K^{-4}}$
τ	Electricity consumption to pump one cubic meter of sludge to an AB or an HT device	$\mathrm{kJ\cdot m^{-3}_{Sludge}}$
φ	Electricity consumption of the membrane modules separating biomethane and carbon dioxide in the biogas at 35 °C and 1 atm	$\mathrm{kJ\cdot m^{-3}_{Biogas}}$
φ_{eh}	Eelectricity conversion efficiency of an electric heater	%
φ_{ex}	Heat recovery efficiency of a heat exchanger	%
$\varphi_{p/m/s}$	Electricity conversion efficiency for pumping sludge, mixing sludge, separating biomethane and carbon dioxide in the biogas, or liquefying carbon dioxide gas	%
χ	Thermal conductivity of stainless steel	$\mathrm{W\cdot m^{-1}\cdot K^{-1}}$
ψ	Electricity consumption for liquifying carbon dioxide gas	$\mathrm{kJ\cdot kg^{-1}_{CO_2}}$
ω	Electricity consumption to mix one cubic meter of sludge in an AB or an HT device	$\mathrm{kJ\cdot m^{-3}_{Reactor}\cdot d^{-1}}$

1. Introduction

Water resource recovery facilities (WRRFs) produce excessive municipal sewage sludge [1,2]. Sewage sludge is the residual solids with a high water content separated from municipal wastewater during sewage treatment [3,4]. Municipal sludge comprises primary sludge (PS; generated during primary treatment), waste activated sludge (WAS; generated during biological treatment), or their blend. Sewage sludge harms the environment and needs to be treated before disposal or land application [5,6]. Conversely, sewage sludge is a source of value-added products such as biogas (e.g., biomethane), biofuels, and fertilizers [7,8]. Anaerobic digestion (AD), involving organic matter degradation and biomethane production, is a common means to stabilize sewage sludge, reduce its odor, inactivate pathogens, and convert organic matter to a renewable energy source or biomethane [9–11]. Hydrolysis, acidogenesis, acetogenesis, and methanogenesis are the four key steps of AD [12,13]. Hydrolysis by microbial extracellular enzymes solubilizes insoluble or particulate organic matter, such as polysaccharides, proteins, and lipids [14]. Hydrolysis also breaks down large complex soluble organic molecules into smaller molecules [15]. Hydrolysis of complex (soluble or insoluble) organic matter produces simpler organic substances, which can be readily metabolized by wastewater microbes [16,17]. Microbial hydrolysis of complex organic matter is slow [18,19]. Sewage sludge has complex floc structures and hard cell walls [20,21] and more particulate organic matter such as microbial cellular constituents than soluble organic substrates [22]. Therefore, hydrolysis is the rate-controlling step for AD of sewage sludge [23,24].

Physical, chemical, and biological pre-treatment methods can accelerate the hydrolysis of complex organic matter in municipal sludge [21,25]. These methods disrupt cell wall and membrane; degrade extracellular polymeric substances; and convert complex (especially particulate) organic matter to simple, readily biodegradable substrates. Among these methods, hydrothermal treatment (HT) is effective in accelerating hydrolysis, increasing biogas production during AD, dewatering sludge, and killing pathogens [26,27]. HT is also feasible to scale up and use in commercial applications such as the CAMBI™ process [28,29]. HT is a general process using water as the reaction medium at high temperature and pressure to treat, convert, transform, or valorize waste organic matter or biomass [30,31]. In this work, HT refers to incubating municipal sewage sludge under elevated temperature and pressure to break down complex organic matter to facilitate the coupled AD. This study does not consider other forms of HT aiming to directly produce value-added products, such as hydrothermal gasification, hydrothermal carbonization, and hydrothermal liquefaction [32–34].

HT-coupled AD has three configurations. HT is usually applied in a pre-stage system (HT→AD) [23,27,35]. This process uses elevated temperature and pressure to break down complex (especially particulate) organic matter in raw sewage sludge, while simple, readily biodegradable organic matter undergoes the same process. However, HT does not enhance biomethane production from readily biodegradable organic substrates [36]. In addition, residual organic matter in the anaerobic digestate of sludge is mainly particulate and hardly biodegradable. The digestate is thus an ideal feedstock of HT. After HT, the anaerobic digestate can undergo AD for additional biomethane production [37]. Therefore, an inter-stage system (1st AD→HT→2nd AD) and a post-stage/recycle system (AD↔HT) are also possible [38,39]. In the inter-stage system, an anaerobic bioreactor (AB; the 1st AD) first digests sewage sludge and converts readily biodegradable organic matter to biogas [36,39,40]. HT then increases the biodigestibility of the leftover, hardly biodegradable organic matter in the digestate. A separate bioreactor (2nd AD) digests the effluent of HT to produce additional biomethane. In the post-stage/recycle system, an AB digests sludge, the digestate undergoes HT, and the digestate after HT is recirculated to the same bioreactor [41–43]. The inter-stage and post-stage/recycle systems are more effective in enhancing biomethane production during AD than the pre-stage system [36,39,44]. Therefore, the inter-stage and post-stage/recycle systems are promising for municipal sewage sludge treatment and renewable energy production.

HT promotes the production of biomethane from municipal sewage sludge during AD but consumes much energy because of the high specific heat of sludge (close to liquid water) [26,45,46]. Therefore, in a meaningful HT-coupled AD system, the energy gain from enhanced biomethane production must at least offset the energy consumption of HT [47]. Previous studies determined the energy balance of HT-coupled AD systems treating organic wastes [27,48–50]. However, most studies focused on the pre-stage system [46,47,51], and only few studies assessed the energy balance of the inter-stage and post-stage/recycle systems [38–40,52]. A comparison of the energy and economic aspects of these alternative processes is also missing.

Existing energy balance assessments of HT-coupled AD systems are oversimplified. For instance, they omit certain important energy components such as heat gain from anaerobic fermentation (the conversion of organic matter to various products by microbes and biomass synthesis in the absence of oxygen gas) and solar radiation [40,48,50,51]. These energy components are important in the overall energy balance [53]. In addition, existing assessments are primarily for batch systems [39,40,54], whereas full-scale sewage sludge treatment is under continuous flow conditions. However, the energy and economic aspects of continuous flow, HT-coupled AD systems are rarely assessed [48,50,55]. To date, Chen et al. [40] performed the most comprehensive energy balance assessment of HT-coupled AD systems. Nonetheless, that work contains multiple serious mistakes and reaches misleading conclusions.

Existing energy balance assessments of HT-coupled AD systems fail to consider the environmental and economic benefits of capturing and valorizing carbon dioxide in the biogas [40]. Carbon dioxide is valuable in the food and beverage industry and can be purified from the biogas with membrane technology [56]. Capturing carbon dioxide from the biogas reduces greenhouse gas emissions and has economic benefits [57].

This work aims to comprehensively assess the energy and economic aspects of three continuous flow, HT-coupled AD processes plus a control for municipal sewage treatment: a control (AD only), a pre-stage system (HT→AD), an inter-stage system (1st AD→HT→2nd AD), and a post-stage/recycle system (AD↔HT). Several critical energy elements omitted in previous studies, such as heat liberated during anaerobic fermentation, are analyzed in this study. In addition, this work aims to determine the economic benefits of capturing and valorizing carbon dioxide from the biogas in the HT-coupled AD processes. This work hypothesizes that the large energy consumption of HT may challenge the overall energy and economic neutrality in the HT-coupled AD systems. However, capturing and valorizing carbon dioxide from the biogas may offset the energy burden of HT to some extent and achieve a more positive economic gain. Through comprehensive energy and economic assessments, this work contributes to the field by pointing out that using electricity or fossil fuels to conduct HT is unwise economically because of its large energy consumption. Under many scenarios, the use of electricity or fossil fuels to conduct HT results in energy and/or economic loss (i.e., extra energy gained through enhanced biomethane production cannot offset the energy consumption of HT). Therefore, innovative means, such as centrifugation of sludge and direct solar energy, should be used to reduce the energy burden of HT. This work also contributes to the field by proving that capturing carbon dioxide from the biogas is economically beneficial, thus encouraging future studies to consider recovering carbon dioxide from the AD of organic wastes. Finally, by analyzing the net energy and economic outputs of the alternative HT-coupled AD processes, this work indicates that the post-stage/recycle system has more significant economic benefits than the other systems. Therefore, the post-stage/recycle process is the preferred choice in designing future HT-coupled AD systems for municipal sewage sludge treatment. Conversely, the inter-stage system should be avoided because it is more complex to maintain, requires a larger footprint, and offers less significant economic benefits [38]. The equations for the energy and economic analysis in this study are valid for the HT-coupled AD systems of not only municipal sewage sludge but also other types of organic wastes such as agricultural waste, food waste, forestry waste, and industrial organic byproducts. By addressing the fundamentals of energy efficiency and economic viability in the waste-to-energy processes (i.e., HT-coupled AD systems), this work contributes to the development of sustainable solutions for organic waste management across sectors and geographical regions. In summary, this work covers the technical, energy, economic, and environmental aspects (viability and benefits) of implementing HT to enhance the AD of municipal sewage sludge.

2. Methods

2.1. Configurations of hydrothermal-treatment-coupled anaerobic digestion systems

Three conceptual HT-coupled AD systems (Fig. 1B, 1C, and 1D) are considered that treat municipal sewage sludge (PS, WAS, or the blend) in a full-scale WRRF for organic matter degradation and biogas production. An AD-only control (Fig. 1A) is also analyzed. In each configuration, polyimide hollow fiber membrane modules separate biomethane and carbon dioxide from the biogas [56]. After liquefaction, the purified carbon dioxide can be sold to the food and beverage industry for economic benefits.

In the control (Fig. 1A), the raw sludge first passes through heat exchanger 1, which recovers the heat from the effluent of AB 1. The pre-heated sludge is then digested in AB 1. Combined heat and power (CHP) unit 1 (a cogeneration internal combustion engine) produces heat and electricity by burning biomethane.

In the pre-stage system (HT→AD) (Fig. 1B), the raw sludge first passes through heat exchangers A and B, which recover the heat from the effluent of AB A and HT device A, respectively. The pre-heated sludge passes through HT device A and is subsequently digested in AB A. CHP unit A produces heat and electricity by burning biomethane.

In the inter-stage system (1st AD→HT→2nd AD) (Fig. 1C), the raw sludge first passes through heat exchanger I, which captures the heat of the digestate from AB II. The pre-heated sludge is then digested in AB I. The digestate from AB I sequentially passes through heat exchanger II and HT device I. Heat exchanger II captures the heat from the effluent of HT device I, while HT device I increases the biodegradability of the digestate. Finally, the hydrothermally treated sludge is digested in AB II. CHP unit I produces heat and electricity by burning the biomethane from both AB I and AB II.

In the post-stage/recycle system (AD↔HT) (Fig. 1D), the raw sludge first passes through heat exchanger i, which captures the heat of the effluent from AB i. The pre-heated sludge is then digested in AB i. The digestate from AB i sequentially passes through heat exchanger ii and HT device i. Heat exchanger ii captures the heat from the effluent of HT device i, while HT device i increases the biodegradability of the digestate. The hydrothermally treated sludge is recirculated to AB i at a recirculation ratio of 100%. CHP unit i burns biomethane for heat and electricity production.

In each configuration, the CHP unit burns the purified biomethane for heat and electricity, whereas a carbon dioxide recovery unit further upgrades the purified carbon dioxide from the membrane modules to food-grade. During the combustion of biomethane, the CHP unit produces carbon dioxide and water vapor $[CH_{4(g)} + 2O_{2(g)} = CO_{2(g)} + 2H_2O_{(g)}]$. The water vapor is removed from the produced carbon dioxide gas, which is then recirculated to the raw biogas for maximum carbon dioxide production. The heat generated from the CHP unit is recovered via heater exchangers. The recovered heat can compensate for the heat consumption of the AB(s): Heat exchangers 2 and 3 heat AB 1 in the control. Heat exchangers C and D heat AB A in the pre-stage system. Heat exchangers III and IV heat AB I in the inter-stage system. Heat exchangers III and V heat AB II in the inter-stage system. Heat

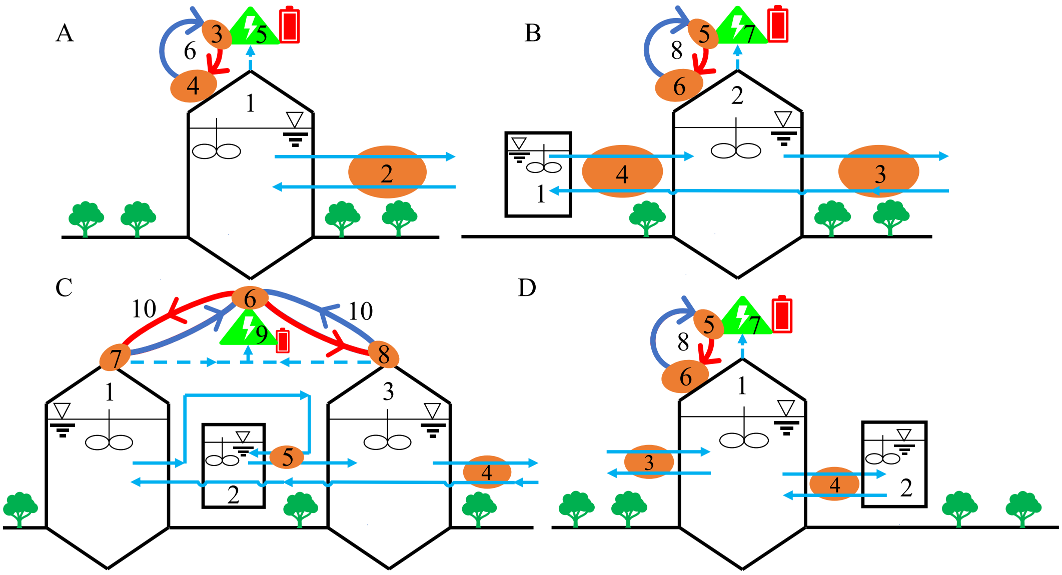

Fig. 1. (A) Control, (B) pre-stage system (HT→AD), (C) inter-stage system (1st AD→HT→2nd AD), and (D) post-stage/recycle system for municipal sewage sludge treatment and biogas production. Solid line (⟶): sludge. Dashed line (- - -→): Biogas. HT: Hydrothermal treatment. AD: Anaerobic digestion. AB: Anaerobic bioreactor. CHP: Combined heat and power. ⬡: AB. ▯: HT device. ⬬: Heat exchanger. ▲: CHP unit. 🔋: Electricity. Fig. 1A: 1: AB 1. 2, 3, and 4: Heat exchangers 1, 2, and 3, respectively. 5: CHP unit 1. 6: Closed-loop water recirculating system (Red curve: water at 90 °C leaving CHP unit 1 to heat AB 1; Blue curve: water at 70 °C returning to CHP unit 1). Fig. 1B: 1: HT device A. 2: AB A. 3, 4, 5, and 6: Heat exchangers A, B, C, and D, respectively. 7: CHP unit A. 8: Closed-loop water recirculating system (Red curve: water at 90 °C leaving CHP unit A to heat AB A; Blue curve: water at 70 °C returning to CHP unit A). Fig. 1C: 1 and 3: ABs I and II, respectively. 2: HT device I. 4, 5, 6, 7, and 8: Heat exchangers I, II, III, IV, and V, respectively. 9: CHP unit I. 10: Closed-loop water recirculating system (Red curve: water at 90 °C leaving CHP unit I to heat ABs I and II; Blue curve: water at 70 °C returning to CHP unit I). Fig. 1D: 1: AB i. 2: HT device i. 3, 4, 5, and 6: Heat exchangers i, ii, iii, and iv, respectively. 7: CHP unit i. 8: Closed-loop water recirculating system (Red curve: water at 90 °C leaving CHP unit i to heat AB i; Blue curve: water at 70 °C returning to CHP unit i).

exchangers iii and iv heat AB i in the post-stage/recycle system. The surplus heat, if any, is sold to the local or national heat networks at a wholesale market price. The electricity generated by the CHP unit in each system is used to pump and mix sludge, operate the membrane modules to separate carbon dioxide and biomethane in the biogas, liquefy carbon dioxide gas, heat the AB(s), and/or heat the HT device. The surplus electricity, if any, is injected into the electricity grid at a wholesale market price.

2.2. Energy and economic considerations

The sludge treatment processes need heat to raise the sludge temperature for AD (the control) or AD and HT (the three HT-coupled AD systems). The processes also require electricity to pump sludge to and mix sludge in the ABs and the HT devices. In addition, the membrane modules separating biomethane and carbon dioxide consume electricity. Carbon dioxide gas liquefication also needs electricity. Each AB and HT device lose heat to the surroundings because they are hotter than the ambient [50,58,59]. Each AB and HT device gain heat from solar radiation through the cover and the wall, whereas they emit radiant energy (i.e., longwave radiation) to the surroundings by their whole surfaces (cover, wall, and floor) [60,61]. In addition, anaerobic fermentation of organic matter liberates heat [62,63]. Furthermore, biomethane, carbon dioxide, and water vapor in the biogas escape from each AB and remove heat [64,65].

The CHP unit in each process produces energy (heat and electricity) when burning biomethane. The produced heat maintains the temperature of the AB(s) in each system via a closed-loop water recirculating system where low-pressure hot water is the heating medium [66,67]. Specifically, two (for the control, the pre-stage system, and the post-stage/recycle system) or three (for the inter-stage system) heat exchangers recover and use the heat from the CHP unit. The first heat exchanger is connected to the CHP unit and heats the low-pressure hot water from 70 to 90 °C. The heat released when the low-pressure hot water cools from 90 to 70 °C is used by the rest heat exchanger(s) to heat the AB(s). If the heat generated from the CHP unit exceeds the heat demand of the AB(s), the surplus heat, if any, can be sold to the local or national heat networks [68]. Electricity generated from the CHP unit pumps and mixes sludge, operates the membrane modules, liquefies carbon dioxide gas, and heats the AB(s) (when the heat from the CHP unit is insufficient) and the HT device. The surplus electricity, if any, can be sold to the local or national electricity grid [69].

Energy recovery is promising to reduce energy demand [40,47]. Thus, heat from the effluent of each AB and each HT device is recovered via heat exchangers when necessary. The captured heat raises the sludge temperature so that the net heat demand of the system can be reduced.

2.3. Development of energy balance relationships and economic analysis

2.3.1. Assumptions for energy and economic assessments

To simplify the energy and economic analysis, this study makes the following assumptions and considerations for each HT-coupled AD system and the control.

(I) Municipal sewage sludge is well-mixed throughout the system. Mass loss due to biogas production and water evaporation in the AB(s) is negligible. Mass loss in the HT device is also ignored. Thus, the volumetric flow rate of sludge (or digestate) of the WRRF is constant throughout the system.

(II) For each sludge treatment unit (AB or HT device), the temperature is uniform (i.e., no temperature gradient inside a unit). The biogas and the sludge in the AB(s) have the same temperature [70]. The sludge also has the same temperature as the wall, floor, and cover of the AB(s) or the HT device. This study ignores the potential heat transfer inside a sludge treatment unit.

(III) The temperatures of ambient air (T_a), ambient soil (T_{so}), raw municipal sewage sludge (T_{sl}), the HT device, and the AB(s) are constant over time. Climatology suggests that the annual average surface air temperature of the world is 287.15 K (14.0 °C) [71]. However, the ambient air temperature is commonly assumed to be 293.15 K (20.0 °C) for municipal sewage treatment [45,72]. This study, therefore, assumes that the ambient air temperature T_a is 293.15 K (20.0 °C). The average annual soil temperature is approximately 2.3 K higher than the ambient air temperature [73]. Thus, this study uses 295.45 K (22.3 °C) as the ambient soil temperature T_{so}. This study also assumes that the temperature of raw municipal sewage sludge T_{sl} is 288.15 K (15.0 °C) [74,75].

(IV) The AB(s) are operated under a steady state. Both the AB(s) and the HT device are continuous flow stirred tank reactors. For conventional AD, the solids retention time (SRT) is between 20 and 30 d with a typical value of 20 d [76–78]. However, for sludge with pre-treatment such as HT, an SRT between 20 and 30 d is too long and might not be necessary [79,80]. Therefore, this study uses 15 d as the fixed SRT (θ_{AD}) for each AB.

(V) Heat transfer is under steady-state conditions for the entire system [60].

(VI) Heat release or consumption associated with the chemical reactions during HT (e.g., the conversion of complex to simple organic matter) is negligible [47].

(VII) The surface of an AB or an HT device is opaque (i.e., transmissivity is zero) [81,82]. Thus, when solar radiation strikes an AB or an HT device, the sunlight is only reflected or absorbed. For each sludge treatment unit (AB or HT device), only the cover and the wall receive solar radiation, while the floor does not. This study assumes that all the absorbed solar radiation is transformed to heat. Other than the radiant energy emitted from an AB or an HT device, radiant energy emitted from other treatment units or compartments (such as a CHP unit and a pump) is negligible. In addition, the energy associated with atmospheric longwave radiation is negligible [60].

(VIII) Pressure for the entire system stays at 101,325 Pa (1 atm) except for the HT device, where the inside pressure is greater than 1 atm when the temperature of the sludge is greater than 100 °C [83,84].

(IX) The HT device and the heat exchangers recovering heat from the sludge do not change the total solids (TS) or volatile solids (VS) concentration of the sludge.

(X) Biogas contains mainly biomethane and carbon dioxide and is saturated with water vapor. Biomethane contains over 95% of methane [85], and this work assumes that biomethane is pure methane for convenience purposes. Other gaseous species in the biogas, such as nitrogen gas, ammonia, and hydrogen sulfide, have a negligible effect on energy balance [86–88]. The components of the biogas are ideal gases.

(XI) The mass ratio of VS to TS (f_{VS}) after AD or HT might decrease [39,89,90]. However, for convenience purposes, this study assumes that f_{VS} does not change throughout the system. The f_{VS} for municipal sewage sludge ranges from 40% to 80% [58,91–94]. This study assigns a typical value (65%) to f_{VS}.

(XII) This study assumes that the heat released from anaerobic fermentation at 25 °C is the same as that at 35 °C.

2.3.2. Energy balance for an anaerobic bioreactor

In all systems, the ABs have the same geometry and other important characteristics. Each AB has a cylinder-shaped body with a cone-shaped cover and a cone-shaped floor (Fig. 2). The floor is underneath the ground and exposed to ambient soil, whereas the wall and the cover are exposed to ambient air. The diameter (D_{AD}) and the side height ($H_{si\text{-}AD}$) of each AB are 30 m and 8 m, respectively. The cover or the floor has a height of 3 m. Thus, the middle height of an AB ($H_{mi\text{-}AD}$) is 14 m. The surface area of the floor or cover ($A_{f/c\text{-}AD}$), the surface area of the wall

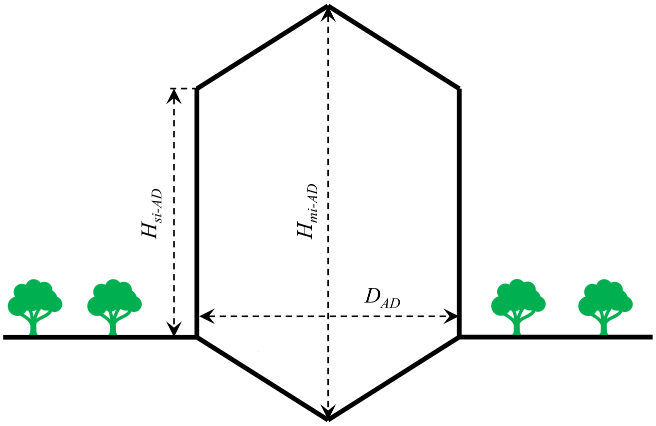

Fig. 2. Geometry of an anaerobic bioreactor. D_{AD}: Diameter. $H_{si\text{-}AD}$: Side height. $H_{mi\text{-}AD}$: Middle height. AD: Anaerobic digestion.

($A_{w\text{-}AD}$), the total (i.e., overall) volume (V_{AD}), and the effective working volume ($V_{e\text{-}AD}$) of each AB are 720.9 m^2 [Equation (1)], 754.0 m^2 [Equation (2)], 7,068.6 m^3 [Equation (3)], and 4,500.0 m^3 [Equation (4)], respectively. The thicknesses of the floor (concrete) or wall (concrete) ($d_{f/w\text{-}AD}$) and cover (fixed concrete) ($d_{c\text{-}AD}$) of each AB are 30.5 and 22.9 cm, respectively [58,95]. This study assumes that the construction material of each AB has the same emissivity coefficient as general concrete (ε_{AD}, 0.85) [96]. In addition, this study uses the typical absorptivity (α_{AD}) of general concrete (0.60) as the absorptivity of the construction material of each AB [97].

$$A_{f/c\text{-}AD} = \pi \cdot \frac{D_{AD}}{2} \cdot \sqrt{\left(\frac{H_{mi\text{-}AD} - H_{si\text{-}AD}}{2}\right)^2 + \frac{D_{AD}^2}{4}} = 720.9\ \text{m}^2 \tag{1}$$

$$A_{w\text{-}AD} = \pi \cdot D_{AD} \cdot H_{si\text{-}AD} = 754.0\ \text{m}^2 \tag{2}$$

$$V_{AD} = \frac{1}{4}\pi \cdot D_{AD}^2 \cdot H_{si\text{-}AD} + \frac{1}{6}\pi \cdot D_{AD}^2 \cdot \left(\frac{H_{mi\text{-}AD} - H_{si\text{-}AD}}{2}\right) = 7,068.6\ \text{m}^3 \tag{3}$$

$$V_{e\text{-}AD} = F \cdot \theta_{AD} = 4,500.0\ \text{m}^3 \tag{4}$$

where F is the volumetric flow rate of sludge for the full-scale WRRF (300 $\text{m}^3_{\text{Sludge}} \cdot \text{d}^{-1}$).

Each AB requires heat ($Q_{k,\ r\text{-}AD\text{-}j}$, $\text{kJ} \cdot \text{d}^{-1}$) to raise the sludge temperature to the mesophilic AD temperature (308.15 K or 35.0 °C) [Equation (5)]. The AB loses heat ($Q_{su\text{-}AD}$, $\text{kJ} \cdot \text{d}^{-1}$) through the floor, wall, and cover because of the temperature difference between the surface and the surroundings [Equation (6)] [64]. An AB also loses heat when biomethane ($Q_{k,\ esm\text{-}AD\text{-}j}$, $\text{kJ} \cdot \text{d}^{-1}$) [Equation (7)], carbon dioxide ($Q_{k,\ esc\text{-}AD\text{-}j}$, $\text{kJ} \cdot \text{d}^{-1}$) [Equation (8)], and water vapor ($Q_{k,\ evw\text{-}AD\text{-}j}$, $\text{kJ} \cdot \text{d}^{-1}$) [Equation (9)] escape [64,65]. The saturation pressure of water vapor in the biogas is calculated with Equation (10). The net radiant energy ($Q_{em\text{-}AD}$, $\text{kJ} \cdot \text{d}^{-1}$) emitted from an AB obeys the Stefan-Boltzmann law [Equation (11)] [81]. The AB consumes electricity to pump sludge ($E_{p\text{-}AD}$, $\text{kJ} \cdot \text{d}^{-1}$) [Equation (12)] and to mix sludge ($E_{m\text{-}AD}$, $\text{kJ} \cdot \text{d}^{-1}$) [Equation (13)] [45].

$$Q_{k,\ r\text{-}AD\text{-}j} = N \cdot F \cdot \left(\rho_{k,\ s,\ AD\text{-}j} \cdot C_{k,\ s,\ AD\text{-}j} \cdot T_{AD} - \rho_{k,\ s,\ AD\text{-}j,\ in} \cdot C_{k,\ s,\ AD\text{-}j,\ in} \cdot T_{k,\ s,\ AD\text{-}j,\ in}\right) \tag{5}$$

where the subscript k equals 1, 2, 3, or 4 (which stands for the control, the pre-stage system, the inter-stage system, or the post-stage/recycle system, respectively); the subscript j equals 1, A, I, II, or i (which stands for AB 1 in the control, AB A in the pre-stage system, AB I in the inter-stage system, AB II in the inter-stage system, or AB i in the post-stage/recycle system, respectively); N equals 1, 0, 1, 0, or 1 when j equals 1, A, I, II, or i, respectively; $\rho_{k,\ s,\ AD\text{-}j}$ [$= \frac{1}{(1 - TS_{k,\ AD\text{-}j})/\rho_w + TS_{k,\ AD\text{-}j}/\rho_{ss}}$] [Equation (5A)] is the mass density of the digestate of AB j in the k^{th} system ($\text{kg}_{\text{Sludge}} \cdot \text{m}^{-3}_{\text{Sludge}}$) [98]; $TS_{k,\ AD\text{-}j}$ is the TS concentration of the digestate of AB j in the k^{th} system (%, percentage of mass); ρ_w is the mass density of the liquid portion of the digestate from an AB (1000 $\text{kg}_{\text{Liquid}} \cdot \text{m}^{-3}_{\text{Liquid}}$); ρ_{ss} is the mass density of dry sludge solids (1400 $\text{kg}_{\text{TS}} \cdot \text{m}^{-3}_{\text{TS}}$) [99]; $C_{k,\ s,\ AD\text{-}j}$ [$= 4.186 \times (1 - 0.812 TS_{k,\ AD\text{-}j})\ \text{kJ} \cdot \text{kg}^{-1}_{\text{Sludge}} \cdot \text{K}^{-1}$] Equation (5B)] is the specific heat capacity of the digestate of AB j in the k^{th} system [65]; 4.816 is the numerical value of the specific heat capacity of water (4.816 $\text{kJ} \cdot \text{kg}^{-1} \cdot \text{K}^{-1}$) [100]; T_{AD} is the mesophilic temperature of AD (308.15 K or 35.0 °C) [101]; $\rho_{k,\ s,\ AD\text{-}j,\ in}$ [$= \frac{1}{(1 - TS_{k,\ AD\text{-}j,\ in})/\rho_w + TS_{k,\ AD\text{-}j,\ in}/\rho_{ss}}$] [Equation (5C)] is the mass density of the influent of AB j in the k^{th} system ($\text{kg}_{\text{Sludge}} \cdot \text{m}^{-3}_{\text{Sludge}}$); $TS_{k,\ AD\text{-}j,\ in}$ is the TS concentration of the influent of AB j in the k^{th} system (%, percentage of mass) [98]; $C_{k,\ s,\ AD\text{-}j,\ in}$ [$= 4.186 \times (1 - 0.812 \text{T}S_{k,\ AD\text{-}j,\ in})\ \text{kJ} \cdot \text{kg}^{-1}_{\text{Sludge}} \cdot \text{K}^{-1}$] [Equation (5D)] is the specific heat capacity of the influent of AB j in the k^{th} system; and $T_{k,\ s,\ AD\text{-}j,\ in}$ is the temperature of the influent of AB j before the heat exchanger in the k^{th} system (K) (the energy balance for the heat exchanger is accounted separately).

$$Q_{su\text{-}AD} = \left[U_{f\text{-}AD} \cdot A_{f/c\text{-}AD} \cdot (T_{AD} - T_{so}) + U_{w\text{-}AD} \cdot A_{w\text{-}AD} \cdot (T_{AD} - T_a) + U_{c\text{-}AD} \cdot A_{f/c\text{-}AD} \cdot (T_{AD} - T_a)\right] \times 86.4\ \text{s} \cdot \text{kJ} \cdot \text{J}^{-1} \cdot \text{d}^{-1} \tag{6}$$

where $U_{f\text{-}AD}$ (0.625 $\text{W} \cdot \text{m}^{-2} \cdot \text{K}^{-1}$), $U_{w\text{-}AD}$ (4.883 $\text{W} \cdot \text{m}^{-2} \cdot \text{K}^{-1}$), and $U_{c\text{-}AD}$ (3.293 $\text{W} \cdot \text{m}^{-2} \cdot \text{K}^{-1}$) are the overall heat transfer coefficients of the floor of the AB in contact with 3-m-thick wet earth, the wall of the AB exposed to ambient air, and the cover of the AB exposed to ambient air, respectively [95]; and 86.4 $\text{s} \cdot \text{kJ} \cdot \text{J}^{-1} \cdot \text{d}^{-1}$ is a unit conversion factor.

$$Q_{k,\ esm\text{-}AD\text{-}j} = V_{e\text{-}AD} \cdot Y_{k,\ j} \cdot MM_m \cdot C_m \cdot (T_{AD} - T_a)/MV \tag{7}$$

where $Y_{k,\ j}$ [$= (TS_{k,\ AD\text{-}j,\ in} \cdot \rho_{k,\ s,\ AD\text{-}j,\ in} - TS_{k,\ AD\text{-}j} \cdot \rho_{k,\ s,\ AD\text{-}j}) \cdot Y_{VS} \cdot f_{VS} \cdot MV/\theta_{AD}$] [Equation (7A)] is the biomethane production rate of AB j in the k^{th} system at 35 °C and 1 atm ($\text{m}^3_{\text{Methane}} \cdot \text{m}^{-3}_{\text{Reactor}} \cdot \text{d}^{-1}$) [102], Y_{VS} is the VS-to-methane conversion factor (27.32 $\text{mol}_{\text{Methane}} \cdot \text{kg}^{-1}\ \text{VS}_{\text{Destructed}}$), MV is the molar volume of any ideal gas at 35 °C and 1 atm (0.0253 $\text{m}^3_{\text{Gas}} \cdot \text{mol}^{-1}$) [103], MM_m is the molar mass of methane (0.016 $\text{kg} \cdot \text{mol}^{-1}$), and C_m is the constant-pressure specific heat capacity of methane at 308.15 K or 35.0 °C (2.247 $\text{kJ} \cdot \text{kg}^{-1}_{\text{Methane}} \cdot \text{K}^{-1}$) [104]. The VS-to-methane conversion factor Y_{VS} is based on the assumptions that I) 1 kg of chemical oxygen demand (COD) destroyed under anaerobic conditions can produce 0.395 m^3 of biomethane at 35.0 °C and 1 atm and II) the VS-to-COD ratio for municipal sewage sludge is 1:1.75 [105–107].

$$Q_{k,\ esc\text{-}AD\text{-}j} = V_{e\text{-}AD} \cdot Y_{k,\ j} \cdot \frac{f_{cd}}{f_m} \cdot MM_c \cdot C_c \cdot (T_{AD} - T_a)/MV \tag{8}$$

where f_{cd} (32%) and f_m (62%) are the volumetric ratios of carbon dioxide and biomethane in the biogas, respectively [3,108]; MM_c is the molar mass of carbon dioxide (0.044 $\text{kg} \cdot \text{mol}^{-1}$); and C_c is the constant-pressure specific heat capacity of carbon dioxide at 308.15 K or 35.0 °C (0.854 $\text{kJ} \cdot \text{kg}^{-1}_{\text{Carbon dioxide}} \cdot \text{K}^{-1}$) [109].

$$Q_{k,\ evw\text{-}AD\text{-}j} = \frac{V_{e\text{-}AD} \cdot Y_{k,\ j} \cdot x_{wv} \cdot MM_w}{f_m \cdot MV} \cdot [(T_{AD} - T_a) \cdot C_{wv} + \Delta H_w] \tag{9}$$

where x_{wv} ($= P_{wv}/101{,}325\ \text{Pa} = 0.055$) is the molar fraction of water vapor in the biogas [110], P_{wv} (5,623 Pa) is the saturation pressure of water vapor in the biogas [Equation (10)] [111–113], MM_w is the molar mass of water (0.018 $\text{kg} \cdot \text{mol}^{-1}$), C_{wv} is the constant-pressure specific heat capacity of water vapor at 308.15 K or 35.0 °C (1.866 $\text{kJ} \cdot \text{kg}^{-1}_{\text{Water vapor}} \cdot \text{K}^{-1}$) [114], and ΔH_w is the enthalpy (heat) of vaporization of water at 308.15 K or 35.0 °C (2,417.9 $\text{kJ}\cdot\text{kg}^{-1}_{\text{Water vapor}}$) [115].

$$\begin{aligned}\log_{10}(P_{wv}/100) = & -7.90298(373.15\ \text{K}/T_{AD} - 1) \\ & + 5.02808\log_{10}(373.15\ \text{K}/T_{AD}) \\ & - 1.3816\left(10^{4.344 - 11.344T_{AD}/373.15\ \text{K}} - 10^{-7}\right) \\ & + 8.1328\left(10^{-3.49149 \times 373.15\ \text{K}/T_{AD} + 0.49149} - 10^{-3}\right) \\ & + \log_{10}1013.25\end{aligned} \tag{10}$$

$$\begin{aligned}Q_{em\text{-}AD} = & \ \sigma\cdot\varepsilon_{AD}\cdot\left[\left(T_{AD}^4 - T_a^4\right)\cdot\left(A_{f/c\text{-}AD} + A_{w\text{-}AD}\right)\right. \\ & \left. + \left(T_{AD}^4 - T_{so}^4\right)\cdot A_{f/c\text{-}AD}\right] \times 86.4\ \text{s}\cdot\text{kJ}\cdot\text{J}^{-1}\cdot\text{d}^{-1}\end{aligned} \tag{11}$$

where σ is the Stefan-Boltzmann constant (5.670×10^{-8} $\text{W}\cdot\text{m}^{-2}\cdot\text{K}^{-4}$) [82].

$$E_{p\text{-}AD} = F\cdot\tau \tag{12}$$

where τ is the electricity consumption to pump one cubic meter of sludge to an AB or an HT device (1800 $\text{kJ}\cdot\text{m}^{-3}_{\text{Sludge}}$) [45,116].

$$E_{m\text{-}AD} = V_{e\text{-}AD}\cdot\omega \tag{13}$$

where ω is the electricity consumption to mix one cubic meter of sludge in an AB or an HT device (300 $\text{kJ}\cdot\text{m}^{-3}_{\text{Reactor}}\cdot\text{d}^{-1}$) [45,116].

The AB gains heat ($Q_{so\text{-}AD}$, $\text{kJ}\cdot\text{d}^{-1}$) from solar radiation through the cover and wall [Equation (14)] [82,117].

$$Q_{so\text{-}AD} = I\cdot\alpha_{AD}\cdot\left(A_{f/c\text{-}AD} + A_{w\text{-}AD}\right) \tag{14}$$

where I is the annual average solar radiation incident on an AB or an HT device (16,000 $\text{kJ}\cdot\text{m}^{-2}\cdot\text{d}^{-1}$). The solar constant (1367 $\text{W}\cdot\text{m}^{-2}$ or 118,109 $\text{kJ}\cdot\text{m}^{-2}\cdot\text{d}^{-1}$) is the radiant solar energy flux received by a plane (with a unit area and normal to the solar radiation) at the outer edge of the atmosphere of Earth [81,118]. Considering that some solar radiation is absorbed by the atmosphere, the cover and wall of an AB or an HT device are not always normal to the solar radiation, and an AB or an HT device does not receive solar radiation at night, we assign a value of 16, 000 $\text{kJ}\cdot\text{m}^{-2}\cdot\text{d}^{-1}$ to I.

Anaerobic fermentation of organic matter is exothermic and releases heat. Therefore, this part of energy should be considered in the energy balance of HT-coupled AD systems [60,65]. This study uses $C_{10}H_{19}O_3N$ with a molar mass of 201.3 $\text{g}\cdot\text{mol}^{-1}$ as the empirical formula of organic matter in municipal sewage sludge [12,119]. This study assumes that I) Microbial cells (microbial organic matter) synthesized during anaerobic fermentation have an empirical formula of $C_5H_7O_2N$ [12]; II) Seven percent (7%) of the electrons provided by the electron donor (i.e., $C_{10}H_{19}O_3N$) are used for biomass (i.e., $C_5H_7O_2N$) synthesis ($f_c = 0.07$) [12]; III) The remaining electrons (93%) are used for energy production at an SRT of 15 d ($f_e = 0.93$); and VI) Carbon dioxide is the terminal electron acceptor, while ammonium is the nitrogen source for anaerobic biosynthesis [3,12,58]. The overall stoichiometric equation of anaerobic fermentation [Equation (15)] for an SRT of 15 d is based on the above assumptions.

The standard enthalpy (heat) of combustion of the dry biomass of bacteria with an empirical formula of $CH_{1.66}O_{0.41}N_{0.21}$ is −521.35 kilojoules per mole of carbon ($\text{kJ}\cdot\text{mol}^{-1}$ C) [120]. This study assumes that the standard enthalpy of combustion of dry anaerobic biomass with an empirical formula of $C_5H_7O_2N$ or $CH_{1.4}O_{0.4}N_{0.2}$ [Equation (16)] is also −521.35 $\text{kJ}\cdot\text{mol}^{-1}$ C. The standard enthalpy of formation of anaerobic biomass ($C_5H_7O_2N$) is then −361.10 $\text{kJ}\cdot\text{mol}^{-1}$ [Equation (17)].

$$\begin{aligned}& C_{10}H_{19}O_3N + 4.8000H_2O_{(l)} \\ & \rightarrow 5.8125CH_{4(g)} + 2.4875CO_{2(g)} + 0.8250HCO^-_{3(aq)} \\ & \quad + 0.8250NH^+_{4(aq)} + 0.1750C_5H_7O_2N\end{aligned} \tag{15}$$

$$C_5H_7O_2N + 5.75O_{2(g)} \rightarrow 5CO_{2(g)} + 3.5H_2O_{(l)} + 0.5N_{2(g)} \tag{16}$$

$$\begin{aligned}\Delta H^\circ_{C_5H_7O_2N\text{-Comb}} & = 3.5\Delta H^\circ_{f\left(H_2O_{(l)}\right)} + 0.5\Delta H^\circ_{f\left(N_{2(g)}\right)} + 5\Delta H^\circ_{f\left(CO_{2(g)}\right)} \\ & \quad -5.75\Delta H^\circ_{f\left(O_{2(g)}\right)} - \Delta H^\circ_{f(C_5H_7O_2N)} \\ & = -521.35 \times 5\text{kJ}\cdot\text{mol}^{-1} \\ & = -2,606.75\ \text{kJ}\cdot\text{mol}^{-1}\end{aligned} \tag{17}$$

where $\Delta H^\circ_{C_5H_7O_2N\text{-Comb}}$ is the standard enthalpy change for the combustion of dry anaerobic biomass $C_5H_7O_2N$ (−2,606.75 $\text{kJ}\cdot\text{mol}^{-1}$), $\Delta H^\circ_{f\left(H_2O_{(l)}\right)}$ is the standard enthalpy of formation of $H_2O_{(l)}$ (−285.80 $\text{kJ}\cdot\text{mol}^{-1}$) [110], $\Delta H^\circ_{f\left(N_{2(g)}\right)}$ is the standard enthalpy of formation of $N_{2(g)}$ (0 $\text{kJ}\cdot\text{mol}^{-1}$), $\Delta H^\circ_{f\left(CO_{2(g)}\right)}$ is the standard enthalpy of formation of $CO_{2(g)}$ (−393.51 $\text{kJ}\cdot\text{mol}^{-1}$), $\Delta H^\circ_{f\left(O_{2(g)}\right)}$ is the standard enthalpy of formation of $O_{2(g)}$ (0 $\text{kJ}\cdot\text{mol}^{-1}$), and $\Delta H^\circ_{f(C_5H_7O_2N)}$ is the standard enthalpy of formation of anaerobic biomass $C_5H_7O_2N$ ($\text{kJ}\cdot\text{mol}^{-1}$).

Sludge organic matter $C_{10}H_{19}O_3N$ has a COD equivalent of 2.11 g $\text{COD}\cdot\text{g}^{-1}$ substrate [Equation (18)]. As a result, during anaerobic fermentation, 13.71 mmol of biomethane is produced when 1.00 g of COD is destroyed [Equation (15)]. The energy contents of PS and WAS samples in India are approximately 21.0 and 17.0 $\text{kJ}\cdot\text{g}^{-1}$ TS or dry weight, respectively [121]. Assuming that the TS-to-COD ratio for sewage sludge is 1.14, the energy contents of PS and WAS samples in India are then approximately 18.5 and 14.9 $\text{kJ}\cdot\text{g}^{-1}$ COD, respectively. In a WRRF in Germany, the energy contents of PS and WAS samples are approximately 13.6 and 14.3 $\text{kJ}\cdot\text{g}^{-1}$ COD, respectively [122]. In municipal WRRFs in Wisconsin (U.S.A.), the energy contents of PS and WAS samples are approximately 15.7 and 16.1 $\text{kJ}\cdot\text{g}^{-1}$ COD, respectively [123]. This study, therefore, uses 15.5 $\text{kJ}\cdot\text{g}^{-1}$ COD (the arithmetic mean value of 18.5, 14.9, 13.6, 14.3, 15.7, and 16.1 $\text{kJ}\cdot\text{g}^{-1}$ COD) as the energy content of organic matter in municipal sewage sludge. Sludge organic matter with an empirical formula of $C_{10}H_{19}O_3N$ can be fully combusted [Equation (18)]. Therefore, the standard enthalpy of formation of sludge organic matter $C_{10}H_{19}O_3N$ is −59.87 $\text{kJ}\cdot\text{mol}^{-1}$ [Equation (19)] [124].

$$C_{10}H_{19}O_3N + 13.25O_{2(g)} \rightarrow 10CO_{2(g)} + 9.5H_2O_{(l)} + 0.5N_{2(g)} \tag{18}$$

$$\begin{aligned}\Delta H^\circ_{C_{10}H_{19}O_3N\text{-Comb}} & = 9.5\Delta H^\circ_{f\left(H_2O_{(l)}\right)} + 0.5\Delta H^\circ_{f\left(N_{2(g)}\right)} + 10\Delta H^\circ_{f\left(CO_{2(g)}\right)} \\ & \quad -13.25\Delta H^\circ_{f\left(O_{2(g)}\right)} - \Delta H^\circ_{f(C_{10}H_{19}O_3N)} \\ & = -EC_{C_{10}H_{19}O_3N} - 2.75\ \text{mol} \times R \times T\end{aligned} \tag{19}$$

where $\Delta H^\circ_{C_{10}H_{19}O_3N\text{-Comb}}$ is the standard enthalpy change for the combustion of dry sludge organic matter $C_{10}H_{19}O_3N$ ($\text{kJ}\cdot\text{mol}^{-1}$) [Equation (18)], $\Delta H^\circ_{f(C_{10}H_{19}O_3N)}$ is the standard enthalpy of formation of sludge organic matter $C_{10}H_{19}O_3N$ ($\text{kJ}\cdot\text{mol}^{-1}$), $EC_{C_{10}H_{19}O_3N}$ is the energy content of sludge organic matter $C_{10}H_{19}O_3N$ (15.5 $\text{kJ}\cdot\text{g}^{-1}$ COD or 6,583.52 $\text{kJ}\cdot\text{mol}^{-1}$), R is the universal gas constant (8.314×10^{-3} $\text{kJ}\cdot\text{mol}^{-1}\cdot\text{K}^{-1}$) [110], and T is the assumed temperature of the standard state condition (298.15 K or 25.0 °C). The −2.75 moles are the sum of the amount (measured in moles) of the produced gases minus the amount (measured in moles) of oxygen gas when one mole of $C_{10}H_{19}O_3N$ is fully combusted [124].

As a result, the standard enthalpy change of anaerobic fermentation of sludge organic matter $C_{10}H_{19}O_3N$ is −724.17 $\text{kJ}\cdot\text{mol}^{-1}$ [Equation (20)], and 124.59 kJ (= 724.17 kJ ÷ 5.8125) of heat (ΔH_m) is liberated when one mole of biomethane is produced. Taken together, anaerobic fermentation [Equation (15)] of sludge organic matter in the HT-coupled AD systems releases significant heat ($Q_{k,\ li\text{-}j}$, $\text{kJ}\cdot\text{d}^{-1}$) [Equation (21)].

$$\begin{aligned}\Delta H^{\circ}_{C_{10}H_{19}O_3N\text{-}AnaFerm} &= 5.8125\Delta H^{\circ}_{f\left(CH_{4(g)}\right)} + 2.4875\Delta H^{\circ}_{f\left(CO_{2(g)}\right)} \\ &+0.8250\Delta H^{\circ}_{f\left(HCO^{-}_{3(aq)}\right)} + 0.8250\Delta H^{\circ}_{f\left(NH^{+}_{4(aq)}\right)} \\ &+0.1750\Delta H^{\circ}_{f(C_5H_7O_2N)} - \Delta H^{\circ}_{f(C_{10}H_{19}O_3N)} - 4.8000\Delta H^{\circ}_{f\left(H_2O_{(l)}\right)}\end{aligned} \tag{20}$$

where $\Delta H^{\circ}_{C_{10}H_{19}O_3N-AnaFerm}$ is the standard enthalpy change for the anaerobic fermentation of organic matter $C_{10}H_{19}O_3N$ ($kJ \cdot mol^{-1}$), $\Delta H^{\circ}_{f\left(CH_{4(g)}\right)}$ is the standard enthalpy of formation of $CH_{4(g)}$ (-74.6 $kJ \cdot mol^{-1}$) [110], $\Delta H^{\circ}_{f\left(HCO^{-}_{3(aq)}\right)}$ is the standard enthalpy of formation of $HCO^{-}_{3(aq)}$ (-692.0 $kJ \cdot mol^{-1}$) [110], and $\Delta H^{\circ}_{f\left(NH^{+}_{4(aq)}\right)}$ is the standard enthalpy of formation of $NH^{+}_{4(aq)}$ (-132.50 $kJ \cdot mol^{-1}$) [110].

$$Q_{k,\ li\text{-}j} = V_{e\text{-}AD} \cdot Y_{k,\ j} \cdot \Delta H_m / MV \tag{21}$$

where $Q_{k,\ li\text{-}j}$ is the heat released from anaerobic fermentation of organic matter within AB j in the k^{th} system at 35 °C.

2.3.3. Energy balance for a hydrothermal treatment device

Each HT device is cylindrical (Fig. 3) with a diameter (D_{HT}) of 4 m and a height (H_{HT}) of 1.4 m. The HT device is above ground and exposed to ambient air. The total surface area (A_{HT}), floor area ($A_{f\text{-}HT}$), total volume (V_{HT}), and effective working volume ($V_{e\text{-}HT}$) of the HT device are 42.7 m^2 [Equation (22)], 12.6 m^2 [Equation (23)], 17.6 m^3 [Equation (24)], and 12.5 m^3 [Equation (25)], respectively. The average retention time (t_{HT}) of sludge in the HT device is 1 h or 0.042 d [15,125]. The thickness of the floor, wall, or cover of the HT device (d_{HT}) is 25.4 cm. The construction material (weathered stainless steel) of the HT device has an emissivity coefficient ε_{HT} of 0.85 [96,126]. In addition, this study assumes that the absorptivity (α_{HT}) of the construction material of the HT device is 0.60 [127]. Stainless steel has a thermal conductivity (χ) of approximately 16.0 $W \cdot m^{-1} \cdot K^{-1}$ [70,128,129]. The convective heat transfer coefficient (h_a) between still air and stainless steel (natural or free convection) is 25.3 $W \cdot m^{-2} \cdot K^{-1}$ [130]. This study assumes that the convective heat transfer coefficient (h_{sl}) between sludge and stainless steel (forced convection) is close to that between thin sludge and hot water coils in anaerobic digesters, which is approximately 170.3 $W \cdot m^{-2} \cdot K^{-1}$ [95]. This study calculates the overall heat transfer coefficient (U_{HT}) of the construction material of the HT device (25.4-cm-think stainless steel) to be 16.32 $W \cdot m^{-2} \cdot K^{-1}$ [Equation (26)] [131,132].

$$A_{HT} = 2 \times \frac{1}{4}\pi \cdot D_{HT}^2 + \pi \cdot D_{HT} \cdot H_{HT} = 42.7\ m^2 \tag{22}$$

$$A_{f\text{-}HT} = \frac{1}{4}\pi \cdot D_{HT}^2 = 12.6\ m^2 \tag{23}$$

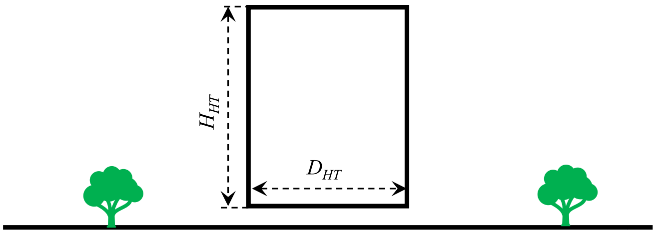

Fig. 3. Geometry of a hydrothermal treatment (HT) device. H_{HT}: Side height. D_{HT}: Diameter.

$$V_{HT} = \frac{1}{4}\pi \cdot D_{HT}^2 \cdot H_{HT} = 17.6\ m^3 \tag{24}$$

$$V_{e\text{-}HT} = F \cdot t_{HT} = 12.5\ m^3 \tag{25}$$

$$\frac{1}{U_{HT}} = \frac{1}{h_a} + \frac{d_{HT}}{\chi} + \frac{1}{h_{sl}} \tag{26}$$

The HT device requires heat ($Q_{k,\ r\text{-}HT}$, $kJ \cdot d^{-1}$) to raise the sludge temperature to the target HT temperature [Equation (27)] [55,133]. The HT device loses heat ($Q_{su\text{-}HT}$, $kJ \cdot d^{-1}$) because of the temperature difference between the surface and the surroundings [Equation (28)] [58, 64]. The HT device also emits radiant energy ($Q_{em\text{-}HT}$, $kJ \cdot d^{-1}$) [Equation (29)] [81]. In addition, the HT device requires electricity to pump sludge ($E_{p\text{-}HT} = E_{p\text{-}AD}$, $kJ \cdot d^{-1}$) [Equation (12)] and to mix sludge ($E_{m\text{-}HT}$, $kJ \cdot d^{-1}$) [Equation (30)] [45]. The HT device gains heat ($Q_{so\text{-}HT}$, $kJ \cdot d^{-1}$) from solar radiation through its cover and wall [Equation (31)] [82,117].

$$Q_{k,\ r\text{-}HT} = F \cdot \rho_{k,\ s,\ HT} \cdot C_{k,\ s,\ HT} \cdot \left(T_{HT} - T_{k,\ s,\ HT,\ in}\right) \tag{27}$$

where $\rho_{k,\ s,\ HT}$ is the mass density of the influent and effluent of the HT device in the k^{th} system ($kg_{Sludge} \cdot m^{-3}_{Sludge}$), $C_{k,\ s,\ HT}$ is the specific heat capacity of the influent and effluent of the HT device in the k^{th} system ($kJ \cdot kg^{-1}_{Sludge} \cdot K^{-1}$), T_{HT} is the target HT temperature (K), and $T_{k,\ s,\ HT,\ in}$ is the temperature of the influent of the HT device before the heat exchanger in the k^{th} system (K) (the energy balance for the heat exchanger is accounted separately). Specifically, $Q_{1,\ r\text{-}HT}$ is 0 $kJ \cdot d^{-1}$ as the control does not use HT.

$$Q_{su\text{-}HT} = U_{HT} \cdot A_{HT} \cdot (T_{HT} - T_a) \times 86.4\ s \cdot kJ \cdot J^{-1} \cdot d^{-1} \tag{28}$$

$$Q_{em\text{-}HT} = \sigma \cdot \varepsilon_{HT} \cdot \left(T_{HT}^4 - T_a^4\right) \cdot A_{HT} \times 86.4\ s \cdot kJ \cdot J^{-1} \cdot d^{-1} \tag{29}$$

$$E_{m\text{-}HT} = V_{e\text{-}HT} \cdot \omega \tag{30}$$

$$Q_{so\text{-}HT} = I \cdot \alpha_{HT} \cdot \left(A_{HT} - A_{f\text{-}HT}\right) \tag{31}$$

2.3.4. Energy balance for a combined heat and power unit

Of the total energy produced from the CHP unit in the k^{th} system, 10% is lost to the surroundings, 55% (heat conversion efficiency, η_h) is available as heat ($Q_{k,\ CHP}$, $kJ \cdot d^{-1}$) [Equation (32)], and 35% (electricity conversion efficiency, η_e) is available as electricity ($E_{k,\ CHP}$, $kJ \cdot d^{-1}$) [Equation (33)] [55]. Studies used different electricity conversion efficiencies for CHP units, such as 35% [133–135], 40% [136], and 42% [44]. This study uses a typical electricity conversion efficiency of 35%.

$$Q_{k,\ CHP} = Y_k \cdot V_{k,\ e\text{-}AD} \cdot \xi \cdot (1 - \mu) \cdot \eta_h / MV \tag{32}$$

where Y_k is the overall biomethane production rate of the k^{th} system at 35 °C and 1 atm ($m^3_{Methane} \cdot m^{-3}_{Reactor} \cdot d^{-1}$), $V_{k,\ e\text{-}AD}$ is the total effective working volume of the AB(s) in the k^{th} system ($m^3_{Reactor}$), ξ is the lower heating value of methane (801.8 $kJ \cdot mol^{-1}_{Methane}$) [58,137–139], and μ (2%) is the energy loss of the CHP unit when cooling the biogas to remove water vapor for corrosion control [58].

$$E_{k,\ CHP} = Y_k \cdot V_{k,\ e\text{-}AD} \cdot \xi \cdot (1 - \mu) \cdot \eta_e / MV \tag{33}$$

2.3.5. Heat recovery through a heat exchanger

Energy recovery from the AB(s) and the HT device is promising in reducing the overall energy demand of an HT-coupled AD system [40]. In each system, a heat exchanger recovers heat ($Q_{k,\ ex\text{-}AD\text{-}j}$, kJ·d^{-1}) from the digestate of AB j in the k^{th} system to heat the sludge and compensate for the heat requirement of the system [Equation (34)] [58,133]. Another heat exchanger in each system recovers heat ($Q_{k,\ ex\text{-}HT}$, kJ·d^{-1}) from the effluent of the HT device [Equation (35)].

$$Q_{k,\ ex\text{-}AD\text{-}j} = F \cdot \rho_{k,\ s,\ AD\text{-}j} \cdot C_{k,\ s,\ AD\text{-}j} \cdot (T_{AD} - T_a) \cdot \varphi_{ex} \tag{34}$$

where the subscript ($k, ex\text{-}AD\text{-}j$) stands for the heat exchanger recovering heat from the digestate of AB j in the k^{th} system. The heat exchangers are heat exchanger 1 for AB 1 in the control, heat exchanger A for AB A in the pre-stage system, heat exchanger I for AB II in the inter-stage system, and heat exchanger i for AB i in the post-stage/recycle system. Specifically, $Q_{3,\ ex\text{-}AD\text{-}I}$ is 0 kJ·d^{-1} as no heat exchanger recovers heat from the digestate of AB I in the inter-stage system. The symbol φ_{ex} (70%) is the heat recovery efficiency of a heat exchanger. Studies used different efficiencies for a heat exchanger, such as 50% [58,59], 80% [140], 85% [40,116], and 87% [141]. This study uses 70% as the heat recovery efficiency of a general heat exchanger.

$$Q_{k,\ ex\text{-}HT} = F \cdot \rho_{k,\ s,\ HT} \cdot C_{k,\ s,\ HT} \cdot (T_{HT} - T_{AD}) \cdot \varphi_{ex} \tag{35}$$

where the subscript ($k, ex\text{-}HT$) is equal to ($1, ex\text{-}HT$), ($2, ex\text{-}HT$), ($3, ex\text{-}HT$), or ($4, ex\text{-}HT$), standing for a non-existing heat exchanger in the control, heat exchanger B in the pre-stage system recovering heat from the effluent of HT device A, heat exchanger II in the inter-stage system recovering heat from the effluent of HT device I, and heat exchanger ii in the post-stage/recycle system recovering heat from the effluent of HT device i, respectively. In particular, $Q_{1,\ ex\text{-}HT}$ is 0 kJ·d^{-1} since the control does not have an HT device.

Heat exchangers recover heat ($Q_{k,\ exs\text{-}CHP}$, kJ·d^{-1}) [Equation (36)] released from burning biomethane in the CHP unit in each system. The recovered heat can be used to heat the AB(s). These heat exchangers are heat exchangers 2 and 3 in the control; heat exchangers C and D in the pre-stage system; heat exchangers III, IV, and V in the inter-stage system; and heat exchangers iii and iv in the post-stage/recycle system. Even though the inter-stage system has three heat exchangers recovering heat from the CHP unit, the overall heat recovery efficiency is still φ_{ex}^2 [110].

$$Q_{k,\ exs\text{-}CHP} = Q_{k,\ CHP} \cdot \varphi_{ex}^2 \tag{36}$$

2.3.6. Energy balance and economic analysis for the entire systems

To analyze the energy balance of each system, this work calculates the overall heat demand of the AB(s) ($Q_{k,\ de\text{-}AD}$, kJ·d^{-1}) and the HT device ($Q_{k,\ de\text{-}HT}$, kJ·d^{-1}). In each system, heat released from the CHP unit supports the heat demand of the AB(s) via heat exchangers. When the heat generated from the CHP unit is greater than the heat demand of the AB(s) or heat is not required to support the AB(s), the surplus heat from the CHP unit can be sold to the local or national heat networks at a wholesale market price ($P_{h\text{-}s}$) of $2.758 × 10^{-6} kJ^{-1}. The wholesale price of the surplus heat is based on the expected 2023 natural gas spot price at the national benchmark Henry Hub in Louisiana (U.S.A.) of $2.91 MMBtu^{-1} [142]. The price is close to the volumetric weighted mean index price for natural gas of $3.01 MMBtu^{-1} for 2017 in the United States [143].

A portion of the electricity generated from the CHP unit is used to pump and mix sludge ($E_{k,\ CHP\text{-}p/m}$, kJ·d^{-1}) [Equation (37)]. Another portion of the generated electricity is used to separate carbon dioxide and biomethane in the biogas and to liquefy the purified carbon dioxide gas ($E_{k,\ CHP\text{-}sep}$, kJ·d^{-1}) [Equation (38)]. The rest of the generated electricity ($E_{k,\ CHP\text{-}re} = E_{k,\ CHP} - E_{k,\ CHP\text{-}p/m} - E_{k,\ CHP\text{-}sep}$, kJ·d^{-1}) heats the HT device via an electric heater. The rest of the electricity ($E_{k,\ CHP\text{-}re}$) also heats the AB(s) via an electric heater only if the heat from the CHP unit is insufficient to maintain the temperature of the AB(s). If the electricity generated by the CHP unit is greater than the energy demand of the entire system, the surplus electricity is injected into the electricity grid at a wholesale market price ($P_{e\text{-}s}$) of $2.754 × 10^{-5} kJ^{-1}. The wholesale price of the surplus electricity is based on the volumetric weighted mean index price for electricity of $99.159 MWh^{-1} for 2022 in the United States [143]. In addition, this study assumes that the electricity conversion efficiency of an electric heater (φ_{eh}) is 80% [141,144]. Furthermore, this work assumes that the electricity conversion efficiency ($\varphi_{p/m/s}$) for pumping sludge, mixing sludge, separating biomethane and carbon dioxide in the biogas, or liquefying carbon dioxide gas is 70% [145–147].

$$E_{k,\ CHP\text{-}p/m} = \frac{E_{k,\ p/m}}{(1 - \beta) \cdot \varphi_{p/m/s}} \tag{37}$$

where $E_{k,\ p/m}$ (kJ·d^{-1}) is the total electricity demand for pumping and mixing sludge in the k^{th} system; and β (10%) is the overall electricity loss due to transmission and other factors when heating an AB or an HT device, pumping or mixing sludge, separating biomethane and carbon dioxide in the biogas, or liquefying the purified carbon dioxide using the electricity generated from the CHP unit [148–150].

$$E_{k,\ CHP\text{-}sep} = \frac{V_{k,\ e\text{-}AD} \cdot Y_k \cdot \frac{1}{f_m} \cdot \varphi \cdot \lambda}{(1 - \beta) \cdot \varphi_{p/m/s}} + \frac{V_{k,\ e\text{-}AD} \cdot Y_k \cdot \frac{f_{cd}}{f_m} \cdot MM_c \cdot \psi \Big/ MV}{(1 - \beta) \cdot \varphi_{p/m/s}} \tag{38}$$

where φ is the electricity consumption (957.33 kJ·m$^{-3}_{\text{Biogas}}$) of the membrane modules separating biomethane and carbon dioxide in the biogas at 35 °C and 1 atm [56,151]; λ (2.5) is a constant considering that I) The biomethane-rich gas from the first membrane module needs to be purified again in a second membrane module, II) The carbon-dioxide-rich gas from the first membrane module needs to be purified again in a third membrane module, III) Gases rejected by the second and third membrane modules need to be recirculated to the raw biogas, and IV) Extra electricity is needed to remove water vapor from the purified carbon dioxide gas and biomethane; and ψ is the electricity consumption for liquifying carbon dioxide gas (363.89 kJ·kg$^{-1}_{CO_2}$) [152–155].

The overall heat balance (ΔQ_k, kJ·d^{-1}) of the AB(s) in the k^{th} system can be negative, zero, or positive [Equation (39)]. The electricity generated from the CHP unit ($E_{k,\ CHP}$) of the k^{th} system is first used to pump and mix sludge, separate biomethane and carbon dioxide in the biogas, and liquefy carbon dioxide gas. The rest of the electricity ($E_{k,\ CHP\text{-}re}$) is available for maintaining the temperature of the AB(s). The overall electricity balance (ΔE_k, kJ·d^{-1}) of the k^{th} system can be negative, zero, or positive [Equation (40)]. To compute ΔQ_k and ΔE_k, this work considers six scenarios:

Scenario I: The overall heat demand of the AB(s) in the k^{th} system is negative ($Q_{k,\ de\text{-}AD} < 0$). Equation (39A) applies.

Scenario II: The overall heat demand of the AB(s) in the k^{th} system is zero or positive ($Q_{k,\ de\text{-}AD} \geq 0$), but the net heat ($Q_{k,\ exs\text{-}CHP}$) generated from the CHP unit can at least offset the overall heat demand (zero or positive) of the AB(s) ($Q_{k,\ exs\text{-}CHP} - Q_{k,\ de\text{-}AD} \geq 0$). Equation (39B) applies.

Scenario III: The overall heat demand of the AB(s) in the k^{th} system is negative ($Q_{k,\ de\text{-}AD} < 0$). Or, the net heat ($Q_{k,\ exs\text{-}CHP}$) generated from the CHP unit can at least offset the positive (or zero) heat demand of the AB(s) in the k^{th} system ($Q_{k,\ exs\text{-}CHP} - Q_{k,\ de\text{-}AD} \geq 0$). Or, the net heat ($Q_{k,\ exs\text{-}CHP}$) generated from the CHP unit cannot offset the positive heat demand of the AB(s) in the k^{th} system ($Q_{k,\ exs\text{-}CHP} - Q_{k,\ de\text{-}AD} < 0$); and the electricity generated by the CHP unit cannot more than offset the electricity demand of pumping and mixing sludge, separating carbon dioxide and biomethane in the biogas, and liquefying carbon dioxide gas ($E_{k,\ CHP\text{-}re} \leq 0$). Equation (40A) applies.

Scenario IV: The net heat ($Q_{k,\ exs\text{-}CHP}$) generated from the CHP unit cannot offset the positive overall heat demand of the AB(s) in the k^{th} system ($Q_{k,\ exs\text{-}CHP} - Q_{k,\ de\text{-}AD} < 0$), but the net electricity [$E_{k,\ CHP\text{-}re} \cdot (1 - \beta) \cdot \varphi_{eh}$, positive] plus the net heat ($Q_{k,\ exs\text{-}CHP}$) generated from the CHP unit can at least offset the positive heat demand of the AB(s) [$Q_{k,\ exs\text{-}CHP} - Q_{k,\ de\text{-}AD} + E_{k,\ CHP\text{-}re} \cdot (1 - \beta) \cdot \varphi_{eh} \geq 0$]. Equations (39C) and (40B) apply.

Scenario V: The net electricity [$E_{k,\ CHP\text{-}re} \cdot (1 - \beta) \cdot \varphi_{eh}$, positive] plus the net heat ($Q_{k,\ exs\text{-}CHP}$) generated from the CHP unit cannot offset the positive overall heat demand of the AB(s) in the k^{th} system [$Q_{k,\ exs\text{-}CHP} - Q_{k,\ de\text{-}AD} + E_{k,\ CHP\text{-}re} \cdot (1 - \beta) \cdot \varphi_{eh} < 0$]. Equations (39D) and (40C) apply.

Scenario VI: The net heat ($Q_{k,\ exs\text{-}CHP}$) generated from the CHP unit cannot offset the positive overall heat demand of the AB(s) in the k^{th} system ($Q_{k,\ exs\text{-}CHP} - Q_{k,\ de\text{-}AD} < 0$). At the same time, the electricity generated by the CHP unit cannot more than offset the electricity demand for pumping and mixing sludge, separating carbon dioxide and biomethane in the biogas, and liquefying the purified carbon dioxide gas ($E_{k,\ CHP\text{-}re} \leq 0$). Equation (39E) applies.

The net heat ($Q_{k,\ exs\text{-}CHP}$) generated from the CHP unit in each system is always positive. Scenarios I, II, IV, V, and VI are mutually exclusive and are for the heat balance. Scenarios III, IV, and V are for the electricity balance. Scenario III is a combination of Scenarios I, II, and VI. The notation $Q_{k,\ exs\text{-}CHP} - Q_{k,\ de\text{-}AD} \geq 0$ in Equation (40A) denotes the combination of Scenarios I and II.

$$
\begin{aligned}
&\Delta Q_k = Q_{k,\,CHP} > 0 \\
&\text{if } Q_{k,\,de\text{-}AD} < 0 \ \text{39A} \\[2ex]
&\Delta Q_k = Q_{k,\,CHP} - \frac{Q_{k,\,de\text{-}AD}}{\varphi_{ex}^2} = \frac{Q_{k,\,exs\text{-}CHP} - Q_{k,\,de\text{-}AD}}{\varphi_{ex}^2} \geq 0 \\
&\text{if } Q_{k,\,exs\text{-}CHP} - Q_{k,\,de\text{-}AD} \geq 0 \text{ and } Q_{k,\,de\text{-}AD} \geq 0 \ \text{39B} \\[2ex]
&\Delta Q_k = Q_{k,\,exs\text{-}CHP} - Q_{k,\,de\text{-}AD} + E_{k,\,CHP\text{-}re} \cdot (1 - \beta) \cdot \varphi_{eh} \cdot \delta = 0 \\
&\text{if } Q_{k,\,exs\text{-}CHP} - Q_{k,\,de\text{-}AD} < 0 \\
&\text{and } Q_{k,\,exs\text{-}CHP} - Q_{k,\,de\text{-}AD} + E_{k,\,CHP\text{-}re} \cdot (1 - \beta) \cdot \varphi_{eh} \geq 0 \ \text{39C} \\[2ex]
&\Delta Q_k = Q_{k,\,exs\text{-}CHP} - Q_{k,\,de\text{-}AD} + E_{k,\,CHP\text{-}re} \cdot (1 - \beta) \cdot \varphi_{eh} < 0 \\
&\text{if } Q_{k,\,exs\text{-}CHP} - Q_{k,\,de\text{-}AD} + E_{k,\,CHP\text{-}re} \cdot (1 - \beta) \cdot \varphi_{eh} < 0 \\
&\text{and } E_{k,\,CHP\text{-}re} > 0 \ \text{39D} \\[2ex]
&\Delta Q_k = Q_{k,\,exs\text{-}CHP} - Q_{k,\,de\text{-}AD} < 0 \\
&\text{if } Q_{k,\,exs\text{-}CHP} - Q_{k,\,de\text{-}AD} < 0 \text{ and } E_{k,\,CHP\text{-}re} \leq 0 \ \text{39E}
\end{aligned}
\tag{39}
$$

where δ (%) is the percentage of the rest of the electricity from the CHP unit ($E_{k,\ CHP\text{-}re}$) that is used to maintain the temperature of the AB(s) in the k^{th} system. Under Scenarios I, II, and VI (collectively, Scenarios III), δ is 0%. Under Scenario IV, δ is between 0% and 100%. Under Scenario V, δ is 100%.

$$
\begin{aligned}
&\Delta E_k = E_{k,\,CHP\text{-}re} - \frac{Q_{k,\,de\text{-}HT}}{(1 - \beta) \cdot \varphi_{eh}} \\
&\text{if } Q_{k,\,exs\text{-}CHP} - Q_{k,\,de\text{-}AD} \geq 0 \text{ or} \\
&\left(Q_{k,\,exs\text{-}CHP} - Q_{k,\,de\text{-}AD} < 0 \text{ and } E_{k,\,CHP\text{-}re} \leq 0\right) \ \text{40A} \\[2ex]
&\Delta E_k = E_{k,\,CHP\text{-}re} \cdot (1 - \delta) - \frac{Q_{k,\,de\text{-}HT}}{(1 - \beta) \cdot \varphi_{eh}} \\
&\text{if } Q_{k,\,exs\text{-}CHP} - Q_{k,\,de\text{-}AD} < 0 \text{ and} \\
&Q_{k,\,exs\text{-}CHP} - Q_{k,\,de\text{-}AD} + E_{k,\,CHP\text{-}re} \cdot (1 - \beta) \cdot \varphi_{eh} \geq 0 \ \text{40B} \\[2ex]
&\Delta E_k = \frac{-Q_{k,\,de\text{-}HT}}{(1 - \beta) \cdot \varphi_{eh}} \leq 0 \\
&\text{if } Q_{k,\,exs\text{-}CHP} - Q_{k,\,de\text{-}AD} + E_{k,\,CHP\text{-}re} \cdot (1 - \beta) \cdot \varphi_{eh} < 0 \\
&\text{and } E_{k,\,CHP\text{-}re} > 0 \ \text{40C}
\end{aligned}
\tag{40}
$$

The overall economic aspects ($E_{k,\ tot}$, \$$\cdot$d^{-1}) of the k^{th} system are based on the heat and electricity balance of the system [Equation (41)]. For any system, a situation does not exist where the overall heat balance of the AB(s) is negative ($\Delta Q_k < 0$) while the overall electricity balance of the system is positive ($\Delta E_k > 0$).

$$
\begin{aligned}
&E_{k,\,tot} = \Delta E_k \cdot P_{e\text{-}s} + \Delta Q_k \cdot P_{h\text{-}s} \\
&+ V_{k,\,e\text{-}AD} \cdot Y_k \cdot \frac{f_{cd}}{f_m} \cdot MM_c \cdot P_{c\text{-}s} / MV \\
&\text{if } \Delta Q_k \geq 0 \text{ and } \Delta E_k \geq 0 \ \text{41A} \\[2ex]
&E_{k,\,tot} = \Delta E_k \cdot P_{e\text{-}p} + \Delta Q_k \cdot P_{h\text{-}s} \\
&+ V_{k,\,e\text{-}AD} \cdot Y_k \cdot \frac{f_{cd}}{f_m} \cdot MM_c \cdot P_{c\text{-}s} / MV \\
&\text{if } \Delta Q_k \geq 0 \text{ and } \Delta E_k \leq 0 \ \text{41B} \\[2ex]
&E_{k,\,tot} = \Delta E_k \cdot P_{e\text{-}p} + \frac{\Delta Q_k}{(1 - \beta) \cdot \varphi_{eh}} \cdot P_{e\text{-}p} \\
&+ V_{k,\,e\text{-}AD} \cdot Y_k \cdot \frac{f_{cd}}{f_m} \cdot MM_c \cdot P_{c\text{-}s} / MV \\
&\text{if } \Delta Q_k \leq 0 \text{ and } \Delta E_k \leq 0 \ \text{41C}
\end{aligned}
\tag{41}
$$

where $P_{e\text{-}p}$ is the ultimate consumer electricity price for the industrial sector in the United States (\$2.242 × 10^{-5} kJ^{-1}; the arithmetic mean value for the first eight months in 2023) [156] and $P_{c\text{-}s}$ is the stable wholesale market price of food-grade liquid carbon dioxide (\$0.380 kg^{-1}) in the United States [157,158].

3. Results and discussion

3.1. Energy balance of the anaerobic bioreactor(s) and hydrothermal treatment device in each hydrothermal-treatment-coupled anaerobic digestion system

The AB(s) and the HT device in each system are the major units that require energy input. For the AB(s), the electricity demand (to pump and mix sludge) is much less than the heat demand (Fig. 4). The heat demand for the AB(s) is to raise the sludge temperature and to compensate for the heat loss from the escaped biogas, the heat loss due to the temperature difference between the surface of the AB(s) and the surroundings, and the net radiant energy emission. In most cases, the overall heat demand of the AB(s) is negative [Scenario I, Equation (39A), and Table 1], is zero or positive but can be at least offset by the net heat ($Q_{k,\ exs\text{-}CHP}$) generated by the CHP unit [Scenario II, Equation (39B), and Table 1], or is positive but can be at least offset by the positive net electricity [$E_{k,\ CHP\text{-}re} \cdot (1 -$

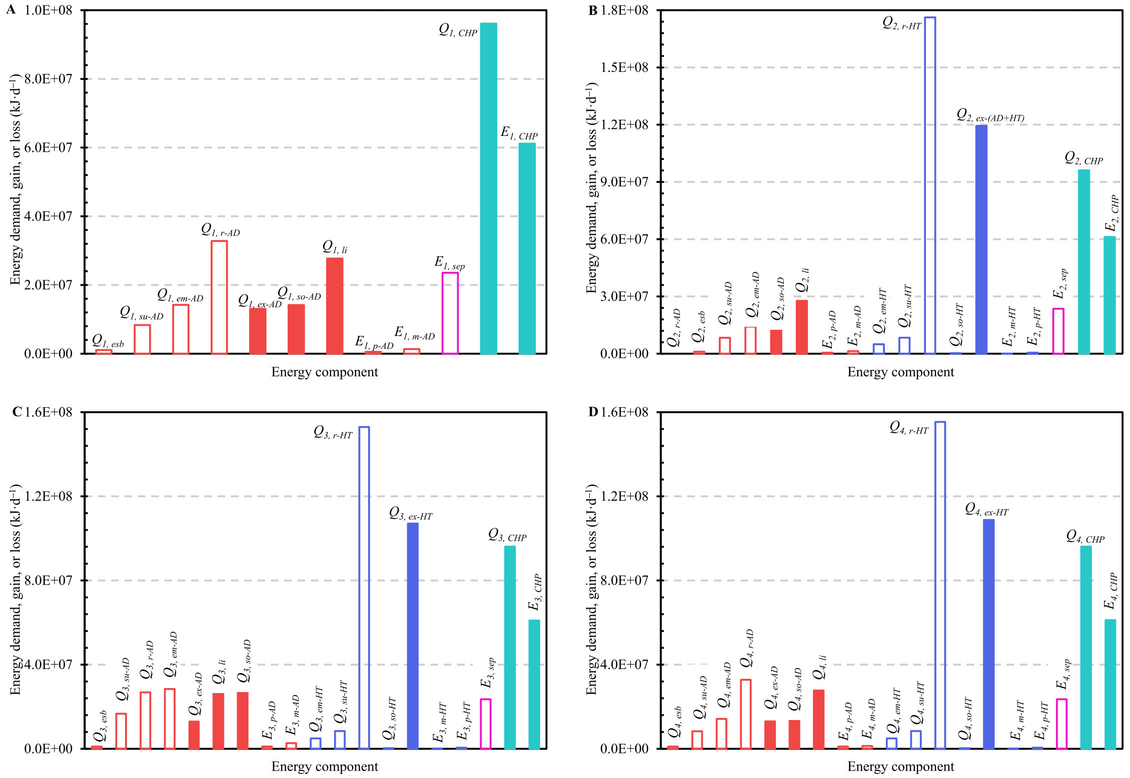

Fig. 4. A snapshot of the energy components of the HT-coupled AD systems and the control treating municipal sewage sludge: (A) Control (AD only), (B) pre-stage system (HT→AD), (C) inter-stage system (1st AD→HT→2nd AD), and (D) post-stage/recycle system (AD↔HT). For all systems, the volumetric flow rate of municipal sewage sludge is 300 $m^3 \cdot d^{-1}$, the total solids (TS) concentration in the raw sludge is 6% (percent of mass), and the overall TS removal is 68%. In the inter-stage system, the TS destruction for the first and second ABs is 20% and 60%, respectively. In the pre-stage system, inter-stage system, and post-stage/recycle system, the HT temperature is 160 °C. AB: Anaerobic bioreactor. AD: Anaerobic digestion. HT: Hydrothermal treatment. CHP: Combined heat and power. The subscript k equals 1, 2, 3, or 4, which stands for the control, pre-stage system, inter-stage system, or post-stage/recycle system, respectively. $Q_{k,\ esb}$: Heat loss due to the escape of biogas (biomethane, carbon dioxide, and water vapor) from the AB(s) in the k^{th} system. $Q_{k,\ su\text{-}AD}$: Heat loss from the surface of the AB(s) due to the temperature difference between the surface and the surroundings in the k^{th} system. $Q_{k,\ em\text{-}AD}$: The net radiant energy emitted from the surface of the AB(s) in the k^{th} system. $Q_{k,\ r\text{-}AD}$: Heat demand to raise the sludge temperature to the temperature of AD (35 °C) in the k^{th} system. $Q_{k,\ ex\text{-}AD}$: Heat recovered from the AB(s) through a heat exchanger in the k^{th} system. $Q_{k,\ ex\text{-}HT}$: Heat recovered from the HT device through a heat exchanger in the k^{th} system. $Q_{k,\ ex\text{-}(AD\ +\ HT)}$: Heat recovered from the AB(s) and the HT device through heat exchangers in the k^{th} system. $Q_{k,\ so\text{-}AD}$: Heat gained from solar radiation through the AB(s) in the k^{th} system. $Q_{k,\ li}$: Heat released during anaerobic fermentation of organic matter in the AB(s) in the k^{th} system. $E_{k,\ p\text{-}AD}$: Electricity demand for pumping sludge into the AB(s) in the k^{th} system. $E_{k,\ m\text{-}AD}$: Electricity demand for mixing sludge in the AB(s) in the k^{th} system. $Q_{k,\ em\text{-}HT}$: The net radiant energy emitted from the surface of the HT device in the k^{th} system. $Q_{k,\ su\text{-}HT}$: Heat loss from the surface of the HT device due to the temperature difference between the surface and the surroundings in the k^{th} system. $Q_{k,\ r\text{-}HT}$: Heat demand to raise the sludge temperature to the HT temperature in the k^{th} system. $Q_{k,\ so\text{-}HT}$: Heat gained from solar radiation through the HT device in the k^{th} system. $E_{k,\ p\text{-}HT}$: Electricity demand for pumping sludge into the HT device in the k^{th} system. $E_{k,\ m\text{-}HT}$: Electricity demand for mixing sludge in the HT device in the k^{th} system. $E_{k,\ sep}$: Electricity demand for I) separating carbon dioxide and biomethane in the biogas and II) liquefying the purified carbon dioxide gas in the k^{th} system. $Q_{k,\ CHP}$: Heat generated from the CHP unit in the k^{th} system. $E_{k,\ CHP}$: Electricity generated from the CHP unit in the k^{th} system. Symbols/notations used in only Fig. 4 are not listed in the Nomenclature section at the begining of this article.

$\beta) \cdot \varphi_{eh}$] plus the net heat ($Q_{k,\ exs\text{-}CHP}$) generated by the CHP unit [Scenario IV, Equation (39C), and Table 1]. For Scenario IV, the net heat ($Q_{k,\ exs\text{-}CHP}$) alone cannot offset the positive overall heat demand of the AB(s) ($Q_{k,\ exs\text{-}CHP} - Q_{k,\ de\text{-}AD} < 0$). In addition, heat absorbed by the AB(s) from solar radiation and liberated by anaerobic fermentation is considerable and can compensate for the heat demand of the AB(s) (Fig. 4). Furthermore, a heat exchanger can recover heat from the digestate of the AB(s). Therefore, in most cases, each system does not require external energy for the heat demand of the AB(s). However, under certain circumstances (i.e., when the TS content in the raw sludge is low and/or when the TS removal is low), the positive overall heat demand of the AB(s) is so large that it cannot be offset by the net electricity [$E_{k,\ CHP\text{-}re} \cdot (1-\beta) \cdot \varphi_{eh}$, positive] plus the net heat ($Q_{k,\ exs\text{-}CHP}$) generated by the CHP unit [Scenario V, Equation (39D), and Table 1]. When the TS content in the raw sludge and the TS removal are both too low, the net heat ($Q_{k,\ exs\text{-}CHP}$) generated by the CHP unit cannot offset the positive overall heat demand of the AB(s), and the rest of the electricity ($E_{k,\ CHP\text{-}re}$) generated by the CHP unit is zero or negative [Scenario VI, Equation (39E), and Table 1].

Compared with the AB(s), the HT device in an HT-coupled AD system consumes much more energy to raise the sludge temperature to the HT temperature (Fig. 4). By contrast, the heat loss from the surface of the HT device (due to net radiant energy emission and the temperature difference between the surface and the surroundings) is much smaller because of the smaller surface area of the HT device. Heat exchangers can recover heat from the digestate of an HT device and an AB to compensate for the heat demand of the HT-coupled AD systems. Solar radiation also heats the HT device. However, because the HT device is small, the heat gained from solar radiation is minimal. Overall, the significant energy demand of the HT device is difficult to satisfy, and external energy input might be required.

Because of the large energy consumption of the HT device, an HT-coupled AD system can easily have a lower net energy output than the control. Interestingly, a recent study found that the net energy output of

Table 1

Extent of total solids (TS) removal for various energy balance scenarios for the three HT-coupled AD processes and the control.

System	TS in raw sludge (%)	Range of TS removal (%) that satisfies:					
		Scenario I	Scenario II	Scenario III	Scenario IV	Scenario V	Scenario VI
Control (AD only)	**2**	N/A	[64, 90]	[20, 26] [64, 90]	[57, 63]	[27, 56]	[20, 26]
	4	N/A	[32, 90]	[32, 90]	[28, 31]	[20, 27]	N/A
	6	[74, 90]	[21, 73]	[21, 90]	20	N/A	N/A
	8	[55, 90]	[20, 54]	[20, 90]	N/A	N/A	N/A
	10	[43, 90]	[20, 42]	[20, 90]	N/A	N/A	N/A
Pre-stage system (HT→AD)	**2**	[66, 90]	[24, 65]	[20, 90]	N/A	N/A	[20, 23]
	4	[33, 90]	[20, 32]	[20, 90]	N/A	N/A	N/A
	6	[22, 90]	[20, 21]	[20, 90]	N/A	N/A	N/A
	8	[20, 90]	N/A	[20, 90]	N/A	N/A	N/A
	10	[20, 90]	N/A	[20, 90]	N/A	N/A	N/A
Inter-stage system (1st AD→HT→2nd AD)	**2**	N/A	[82, 92]	[36, 59] [82, 92]	[78, 82]	[60, 78]	[36, 59]
	4	N/A	[42, 92]	[42, 92]	[40, 42]	[36, 39]	N/A
	6	[78, 92]	[36, 78]	[36, 92]	N/A	N/A	N/A
	8	[60, 92]	[36, 59]	[36, 92]	N/A	N/A	N/A
	10	[49, 92]	[36, 48]	[36, 92]	N/A	N/A	N/A
Post-stage/recycle system (AD↔HT)	**2**	N/A	[64, 90]	[20, 41] [64, 90]	[60, 63]	[42, 59]	[20, 41]
	4	N/A	[32, 90]	20 [32, 90]	[30, 31]	[21, 29]	20
	6	[74, 90]	[21, 73]	[21, 90]	20	N/A	N/A
	8	[55, 90]	[20, 54]	[20, 90]	N/A	N/A	N/A
	10	[43, 90]	[20, 42]	[20, 90]	N/A	N/A	N/A

The ranges of the extent of TS removal are not a function of HT temperature. Separating carbon dioxide from the biogas and liquifying the purified carbon dioxide gas are considered. For the control, the per-stage system, and the post-stage/recycle system, the range of TS removal is 20% to 90%. For the inter-stage system, the TS removal of the first AB is 20%, the TS removal of the second AB ranges from 20% to 90%, and the overall TS removal thus ranges from 36% to 92%. For the inter-stage system, the overall TS removal is reported. **Scenario I**: The overall heat demand of the AB(s) in the k^{th} system is negative ($Q_{k,\ de\text{-}AD} < 0$). **Scenario II**: The overall heat demand of the AB(s) in the k^{th} system is zero or positive ($Q_{k,\ de\text{-}AD} \geq 0$), but the net heat generated from the CHP unit can at least offset the heat demand ($Q_{k,\ exs\text{-}CHP} - Q_{k,\ de\text{-}AD} \geq 0$). **Scenario III**: The overall heat demand of the AB(s) in the k^{th} system is negative ($Q_{k,\ de\text{-}AD} < 0$). Or, the net heat generated from the CHP unit can at least offset the positive (or zero) heat demand of the AB(s) in the k^{th} system ($Q_{k,\ exs\text{-}CHP} - Q_{k,\ de\text{-}AD} \geq 0$). Or, the net heat generated from the CHP unit cannot offset the positive overall heat demand of the AB(s) in the k^{th} system ($Q_{k,\ exs\text{-}CHP} - Q_{k,\ de\text{-}AD} < 0$); and the electricity generated by the CHP unit cannot more than offset the electricity demand of pumping sludge, mixing sludge, separating carbon dioxide and biomethane in the biogas, and liquefying carbon dioxide gas ($E_{k,\ CHP\text{-}re} \leq 0$). **Scenario IV**: The net heat generated from the CHP unit cannot offset the positive overall heat demand of the AB(s) in the k^{th} system ($Q_{k,\ exs\text{-}CHP} - Q_{k,\ de\text{-}AD} < 0$), but the net electricity plus the net heat generated from the CHP unit can at least offset the overall heat demand of the AB(s) [$Q_{k,\ exs\text{-}CHP} - Q_{k,\ de\text{-}AD} + E_{k,\ CHP\text{-}re} \cdot (1-\beta) \cdot \varphi_{eh} \geq 0$]. **Scenario V**: The net electricity (positive) plus the net heat generated from the CHP unit cannot offset the positive overall heat demand of the AB(s) in the k^{th} system [$Q_{k,\ exs\text{-}CHP} - Q_{k,\ de\text{-}AD} + E_{k,\ CHP\text{-}re} \cdot (1-\beta) \cdot \varphi_{eh} < 0$]. At the same time, the electricity generated by the CHP unit can more than offset the electricity demand of pumping sludge, mixing sludge, separating carbon dioxide and biomethane in the biogas, and liquefying carbon dioxide gas in the k^{th} system ($E_{k,\ CHP\text{-}re} > 0$). **Scenario VI**: The net heat generated from the CHP unit cannot offset the positive overall heat demand of the AB(s) in the k^{th} system ($Q_{k,\ exs\text{-}CHP} - Q_{k,\ de\text{-}AD} < 0$). In the meanwhile, the electricity generated by the CHP unit cannot more than offset the electricity demand of pumping sludge, mixing sludge, separating carbon dioxide and biomethane in the biogas, and liquefying carbon dioxide gas ($E_{k,\ CHP\text{-}re} \leq 0$). **AB**: Anaerobic bioreactor. **AD**: Anaerobic digestion. **HT**: Hydrothermal treatment. **CHP**: Combined heat and power. $\boldsymbol{Q_{k,\ de\text{-}AD}}$: The overall heat demand of the AB(s) in the k^{th} system. $\boldsymbol{Q_{k,\ exs\text{-}CHP}}$: The net heat generated from the CHP unit in the k^{th} system, which is always positive. $\boldsymbol{E_{k,\ CHP\text{-}re}}$: The electricity generated by the CHP unit in the k^{th} system minus the electricity demand of pumping sludge, mixing sludge, separating carbon dioxide and biomethane in the biogas, and liquefying carbon dioxide gas. $\boldsymbol{\beta}$: The overall electricity loss due to transmission and other factors when heating an HT device or an AB, pumping or mixing sludge, separating carbon dioxide and biomethane in the biogas, or liquefying carbon dioxide gas. $\boldsymbol{\varphi_{eh}}$: The electricity conversion efficiency of an electric heater. **N/A**: Not applicable.

an HT-coupled AD system can be significantly greater than that of the control [40]. The different conclusion from the previous study is because it made wrong assumptions (such as unreasonably high heat recovery efficiency).

3.2. Environmental and economic benefits of recovering carbon dioxide from the biogas

Carbon dioxide is a major greenhouse gas and causes harmful climate change (e.g., global warming) [159,160]. Currently, carbon dioxide generated from the AD process in WRRFs is directly released into the atmosphere. Thus, the AD process causes significant greenhouse gas emissions [119]. Therefore, this work proposes to recover carbon dioxide from the biogas, upgrade it to food-grade, and use it in the food and beverage industry to reduce the greenhouse gas emissions from WRRFs. Even though carbon dioxide used in the food and beverage industry is eventually released into the atmosphere, recovering carbon dioxide from the biogas can reduce the reliance of the industrial carbon dioxide supply on traditional sources such as fossil fuel combustion, ammonia production, and gasification of solid fuels [56]. As a result, recovering carbon dioxide from the biogas has significant environmental benefits.

Recovering carbon dioxide from the biogas also has economic benefits as the recovered carbon dioxide can be sold to the food and beverage industry [56]. For all the HT-coupled AD systems, the economic benefits of recovering carbon dioxide are significant (Fig. 5). In addition, the higher the TS concentration in the raw municipal sludge, the higher the economic benefit of recovering carbon dioxide would be. For instance, in the pre-stage system, at a TS removal of 60%, the economic benefit of recovering carbon dioxide is $\$313 \cdot \mathrm{d}^{-1}$ (compared with no recovering) when the raw sludge has a TS concentration of 2% (percent of mass) (Fig. 5B). When the TS concentration in the raw sludge increases to 10% (percent of mass), the economic benefit of recovering carbon dioxide rises to $\$1617 \cdot \mathrm{d}^{-1}$ for the pre-stage system with a TS removal of 60%. Altogether, recovering carbon dioxide from the biogas can greatly reduce greenhouse gas emissions, which is in line with the goal of decarbonizing the industrial sector in the U.S., as described in President Biden's *Investing in America* agenda [161].

3.3. Comparing the economic aspects of the alternative hydrothermal-treatment-coupled anaerobic digestion processes for sludge treatment

On the basis of comprehensive energy balance and economic assessments, this work compares the economic aspects of three HT-coupled AD systems: Pre-stage system, inter-stage system, and post-stage/recycle system. At the same TS removal, all three configurations

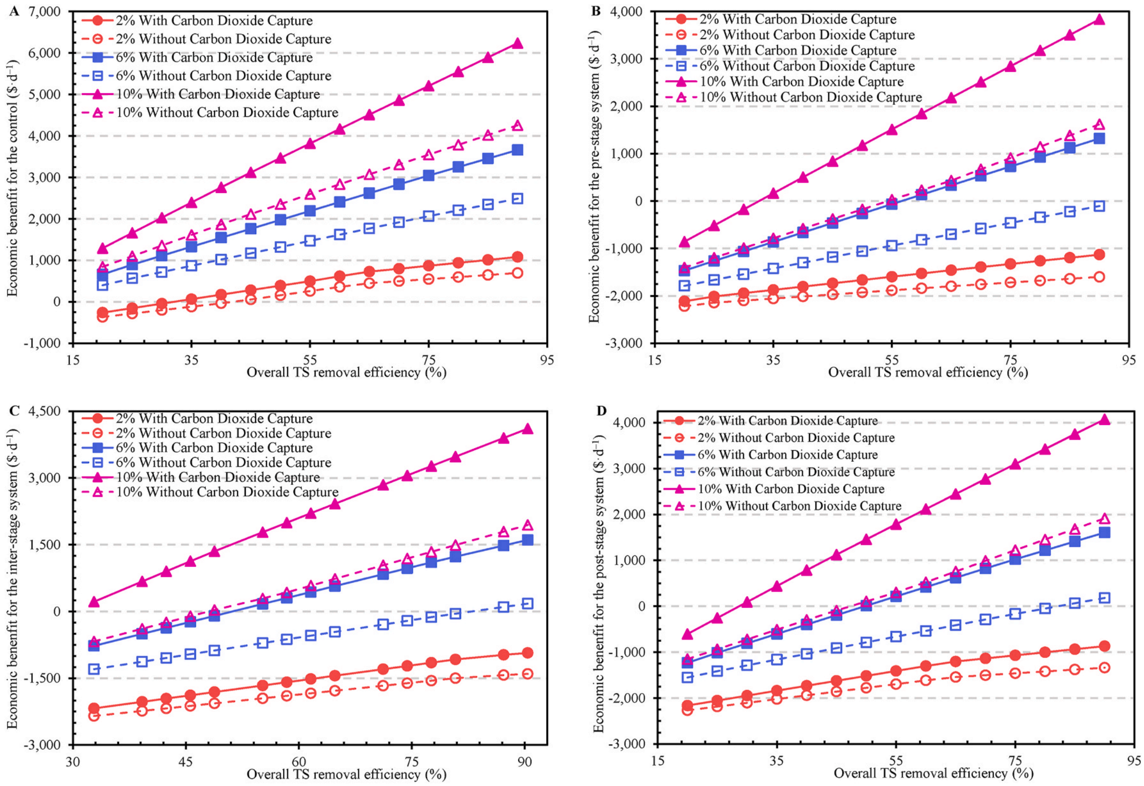

Fig. 5. The economic benefits of the different HT-coupled AD systems and the control treating municipal sewage sludge as a function of the overall total solids (TS) removal: (A) Control (AD only), (B) pre-stage system (HT→AD), (C) inter-stage system (1st AD→HT→2nd AD), and (D) post-stage/recycle system (AD↔HT). For each system, the volumetric flow rate of municipal sewage sludge is 300 $m^3 \cdot d^{-1}$, and two scenarios are considered (i.e., with and without carbon dioxide capture). In the inter-stage system, the TS destruction for the first AB is 20%. For the pre-stage system, inter-stage system, and post-stage/recycle system, the HT temperature is 160 °C. AB: Anaerobic bioreactor. AD: Anaerobic digestion. HT: Hydrothermal treatment. The percentages in the legends: TS concentrations in the raw sludge (percentages of mass).

have much less economic benefits than the control (Fig. 6), indicating that HT demands much energy even with heat recovery (Fig. 4). At the same TS removal, the post-stage/recycle system has a higher economic benefit than the inter-stage system, which, in turn, has a higher economic benefit than the pre-stage system. Therefore, the post-stage/recycle process is the best option for an HT-coupled AD system. Conversely, the inter-stage system should be avoided because it is more complex to maintain, requires a larger footprint, and offers less significant economic benefits [38]. However, the difference in the economic benefits of the three alternative systems is not significant, especially for the inter-stage and post-stage/recycle systems. Considering that the pre-stage system has the simplest configuration and is easy to maintain, it can also be the right choice for municipal sludge treatment and resource recovery [52].

3.4. *Increase in total solids destruction to offset the energy burden of hydrothermal treatment*

HT can enhance the production of biomethane during AD of municipal sewage sludge and other organic wastes [11,105]. However, HT is highly energy demanding [43,45,54] because of the large specific heat capacity of municipal sewage sludge and the high HT temperature applied (usually over 100 °C). The increase in the energy (economic) gain due to the enhanced biogas production after HT should at least offset the energy burden of HT so that incorporating HT in the process is meaningful.

For an HT-coupled AD process, a TS destruction (η_{TS}) exists at which the energy burden of HT can be offset by the enhanced biogas production. This study calculates η_{TS} for the three HT-couple AD processes in four cases: The control (AD only) has a TS destruction of 20% (Case I), 40% (Case II), 60% (Case III), and 80% (Case IV). In each case, the TS concentration of the raw sewage sludge (TS_R; percentage of mass) varies from 2% to 10%, whereas the HT temperature (T_{HT}) varies from 373.15 K (100 °C) to 473.15 K (200 °C). For each combination of TS_R and T_{HT} in each case, this study calculates the overall economic aspects of the four HT-coupled AD systems [Equation (41)] with different TS destruction until the overall economic aspects of the four systems are equal (i.e., $E_{1,\ tot} = E_{2,\ tot} = E_{3,\ tot} = E_{4,\ tot}$). At such TS destruction (η_{TS}, %), the energy burden of HT in an HT-coupled AD system is offset by the increased biogas production (Fig. 7). If an HT-coupled AD system has a TS destruction greater than η_{TS}, the system has a higher economic gain than the control. If an HT-coupled AD process has a TS destruction below η_{TS}, the process has a lower economic gain than the control.

In each case, the values of η_{TS} increase (semi-)linearly with the HT temperature T_{HT} (Fig. 7) with a large slope, indicating that T_{HT} is the key factor affecting the energy balance and economic aspects of an HT-coupled AD process. When T_{HT} is 403.15 K (130 °C) or less, reaching η_{TS} can be practical. However, at higher HT temperatures, the η_{TS} is usually so large that reaching η_{TS} is impossible. For instance, when the control has a TS destruction of 40% and T_{HT} is 433.15 K (160 °C), the η_{TS} for the pre-stage system with a TS_R of 6% (percent of mass) is 95.70% (Fig. 7B). Experimental assessments indicate that an HT-coupled AD system cannot reach such high TS destruction [38,40,48].

The TS concentration in the raw municipal sewage sludge (TS_R) also affects the energy balance and economic aspects of the sludge treatment systems (Fig. 7). The higher TS_R is, the lower η_{TS} is. For instance, when TS_R is 4% (percent of mass), the TS destruction is 40% for the control, and H_{HT} is 393.15 K (120 °C), η_{TS} is 89.02% for the post-stage/recycle system, significantly higher than that ($\eta_{TS} = 72.90\%$) when TS_R is 6% (percent of mass) (Fig. 7B).

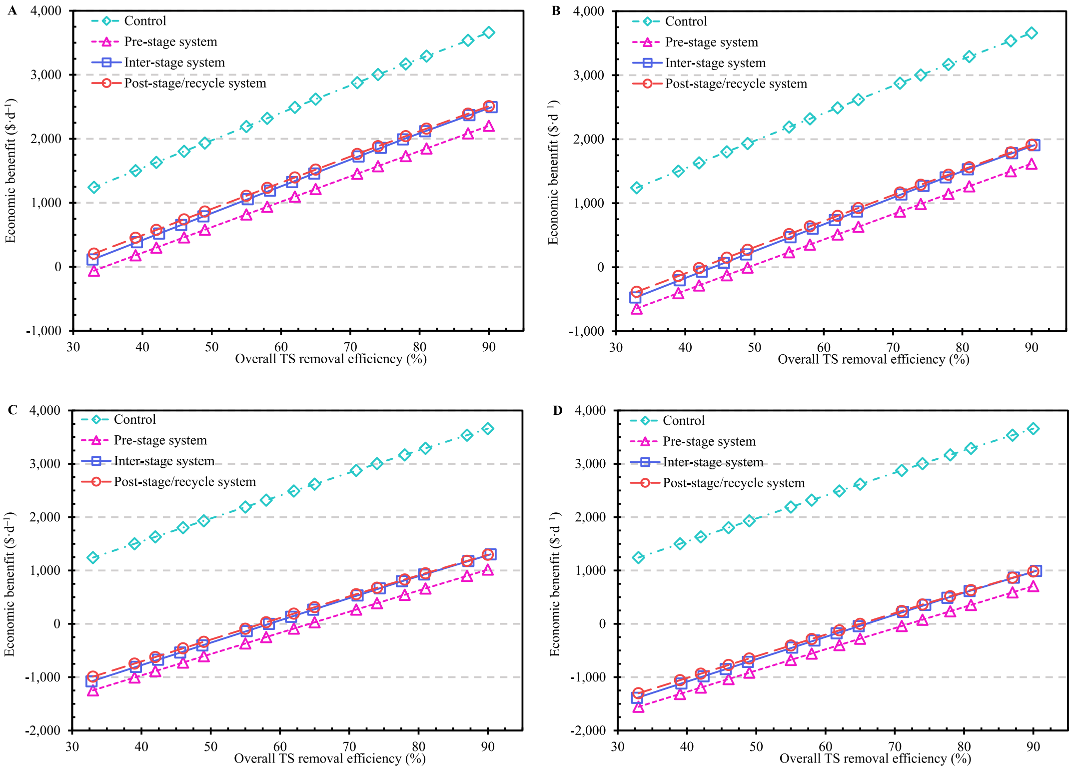

Fig. 6. The economic benefits of the control (AD only), pre-stage system (HT→AD), inter-stage system (1st AD→HT→2nd AD), and post-stage/recycle system (AD↔HT) treating municipal sewage sludge at HT temperatures of (A) 100 °C, (B) 140 °C, (C) 160 °C, and (D) 200 °C. The control does not have an HT device. For each system, the volumetric flow rate of municipal sewage sludge is 300 $m^3 \cdot d^{-1}$, the concentration of total solids (TS) in the raw sludge is 6% (percent of mass), and carbon dioxide capture is considered. In the inter-stage system, the TS destruction for the first AB is 20%. AB: Anaerobic bioreactor. AD: Anaerobic digestion. HT: Hydrothermal treatment.

In addition, the TS destruction of the control determines whether incorporating HT into an AD-based sludge treatment process is economically beneficial. When the control has a low TS destruction (i.e., the sludge has a high content of complex, especially particulate, organic matter that is hardly biodegradable), applying HT is more beneficial (Fig. 7). By contrast, if the control has a high TS destruction, reaching η_{TS} is difficult or even impractical. For instance, when the TS concentration in the raw sludge is 6% (percent of mass) and H_{HT} is 393.15 K (120 °C), η_{TS} for the inter-stage system is 52.74% or 95.58% when the control has a TS destruction of 20% or 60%, respectively (Fig. 7A and Fig. 7C). Removing 52.74% of TS in a well-maintained inter-stage system is practical, but a TS destruction of 95.58% is impossible.

The alternative system configurations have distinct energy and economic aspects. With the same TS concentration in the raw sludge, the same TS destruction of the control, and the same H_{HT}, η_{TS} for the three HT-coupled AD systems is generally in the order of the post-stage/recycle system $<$ the inter-stage system $<$ the pre-stage system (Fig. 7). For comparison, at the same TS removal, the overall economic benefits of the three systems are in the order of the post-stage/recycle system $>$ the inter-stage system $>$ the pre-stage system (Fig. 6). A recent study similarly found that when the recovered energy is used to heat only the AB(s) with surplus heat wasted, the inter-stage system has a higher overall heat output than the pre-stage system [40]. Therefore, the post-stage/recycle system is more economically beneficial.

In summary, the best strategy to apply HT in an AD-based sludge treatment process is using the post-stage/recycle configuration when the raw sludge has a high TS concentration and H_{HT} is low or moderate (i.e., $\leq$ 130 °C). In addition, applying HT is meaningful when the control has a low biogas production (i.e., the raw sludge has a high content of complex, especially particulate, organic matter that is hardly biodegradable). However, when the control has a high TS destruction and/or when the HT temperature is high, the increment in biogas production due to HT cannot offset the energy burden of HT. Overall, the large energy consumption of HT challenges the overall energy and economic neutrality in the HT-coupled AD systems for municipal sewage sludge treatment. Incorporating HT in an AD-based sludge treatment process is economically beneficial only under certain conditions.

3.5. *Potential strategies to increase the energy and economic output of hydrothermal-treatment-coupled anaerobic digestion systems*

Applying HT in AD-based sludge treatment systems to enhance biogas production is a common practice [15,40]. However, under many conditions, the use of HT is not economically beneficial because the energy consumption of HT is huge and cannot be easily offset by the increased biogas production. HT provides multiple advantages to a sludge treatment system such as enhanced pathogen inactivation, increased sludge filterability and dewaterability, promoted recovery of value-added resources, and more pronounced organic matter and solids removal [58,162,163]. Therefore, future studies should reduce the energy burden of HT to increase the energy and economic output of HT-coupled AD systems.

This work proposes three strategies to increase the energy and economic output of an HT-coupled AD system. First, centrifuging sludge can reduce its water content and thus reduce the energy demand of HT if only the concentrated sludge is hydrothermally treated. The specific heat capacity of municipal sludge is high (approximately 4.1 $kJ \cdot kg^{-1} \cdot K^{-1}$, close to liquid water) [164]. Thus, HT consumes significant energy. However, in municipal sewage sludge, most of the complex, hardly biodegradable organic matter is in the solids, whereas the liquid fraction has a lower concentration of total and hardly biodegradable organic matter than the solids [38]. In the liquid fraction, the relative

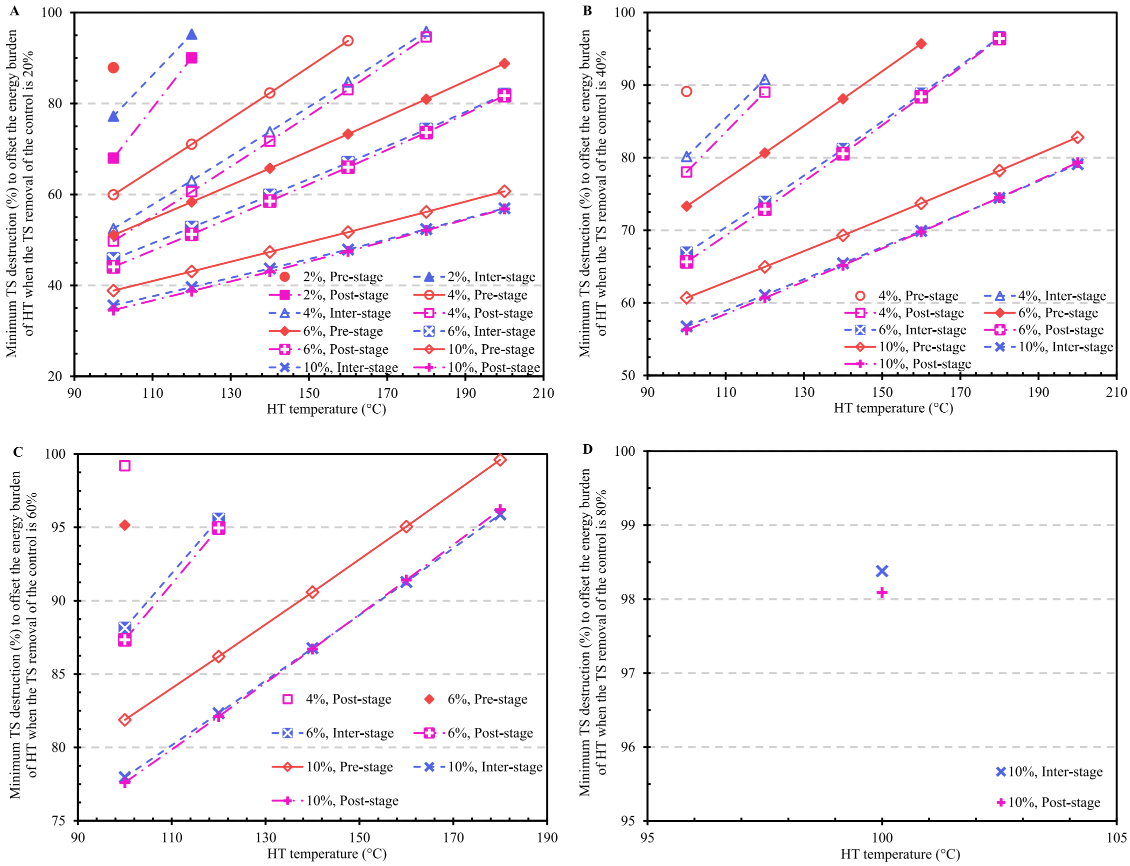

Fig. 7. Minimum total solids (TS) destruction (η_{TS}, %) during anaerobic digestion (AD) of municipal sewage sludge offsetting the energy burden of hydrothermal treatment (HT) when the control has TS destruction of (A) 20%, (B) 40%, (C) 60%, or (D) 80%. The values in the legends indicate the TS concentrations of raw municipal sewage sludge (TS_R; percentage of mass). In the inter-stage system, the first anaerobic bioreactor has a TS removal of 20%. Control: AD only. Pre-stage system: HT→AD. Inter-stage system: 1st AD→HT→2nd AD. Post-stage/recycle system: AD↔HT.

content of readily biodegradable organic matter is high [3,165]. In addition, municipal sewage sludge commonly has a low solids content (i.e., a low TS concentration or a low solids fraction). Therefore, when the raw sludge is hydrothermally treated as a whole, the liquid fraction consumes and wastes most of the heat. This study proposes a strategy to reduce the energy demand of HT: The solids and liquid fractions of the raw sludge should be first separated via centrifugation or other means [45]. Afterward, only the solids fraction is hydrothermally treated. Then, the untreated liquid fraction and the treated solids fraction are combined and used as the feedstock of AD. Since the solids concentration of municipal sludge is usually less than 10% (percent of mass), this strategy can save approximately 80% of the energy demand of HT given that centrifuging sludge consumes a modest amount of energy (144 $kJ\cdot kg^{-1}$ TS or even lower) [166–168]. A recent study proved that with sludge dewatering before AD and HT, an HT-coupled AD system can be promising in energy generation [40].

Second, this work proposes to apply HT to only PS or WAS, mix the hydrothermally treated sludge and the untreated sludge, and digest the blend anaerobically. Municipal WRRFs produce both PS and WAS with production volumes in the same range [169]. Therefore, this strategy can save approximately 50% of the energy demand of HT. However, organic matter in PS is easier to biodegrade during AD than in WAS because of the complex floc structure of WAS [170,171]. Thus, applying HT to only the WAS would be more beneficial [40].

The amount of energy required to raise the sludge temperature to the HT temperature accounts for a significant portion of the total energy demand of an HT-coupled AD system (Fig. 4). Therefore, both strategies (i.e., centrifuging sludge and applying HT to only WAS) can substantially increase the energy and economic output of HT-coupled AD systems.

Third, achieving η_{TS} in a conventional HT-coupled AD system is challenging because the HT device requires significant energy from electricity or fossil fuels to raise the sludge temperature. Because electricity and fossil fuels are not free and have significant environmental burdens, an HT-coupled AD system is less beneficial and less attractive. However, electricity or fossil fuels are not the only energy sources for an HT device. If direct sunlight as a “free,” renewable energy source can be used to conduct HT, HT will become an attractive method to promote the performance of AD. With a modern solar-energy-conversion device, such as a solar evacuated tube collector, raising the temperature of sludge to the HT temperature of up to 200 °C is feasible with direct sunlight [172–174]. This strategy can eliminate the energy reliance on electricity or fossil fuels to raise the sludge temperature to the HT temperature and thus increase the energy and economic output of HT-coupled AD systems for municipal sewage sludge treatment.

3.6. Limitations and sources of error

This work comprehensively analyzes the energy and economic aspects of different HT-coupled AD processes for municipal sewage sludge treatment. Various energy and economic components are considered, and the alternative HT-coupled AD processes are compared. However, this work has four major limitations that should be addressed in future studies. First, the assumptions do not fully reflect the complexity of the HT-coupled AD systems in the real world. This study makes multiple assumptions to simplify the energy and economic analysis. Thus, the analysis might not fully reflect the complex nature of the HT-coupled AD processes. For instance, this study assumes a uniform temperature for each sludge treatment unit such as an AB. However, in the real world, temperature gradients always exist in each unit. In addition, this study assumes that the temperatures of ambient air, ambient soil, raw municipal sewage sludge, each HT device, and each AB are constant over time. However, their temperatures change over time in the real world. Furthermore, this study assumes that an AB and the heat transfer anywhere in any system are both under a steady state, while in the real world, a steady-steady condition rarely exists. This work also ignores the impacts of the organic matter composition (i.e., proportions of different types of organic compounds) of municipal sewage sludge on the performance of the HT-coupled AD systems. Therefore, the analysis does not fully reflect the energy and economic aspects of the HT-coupled AD systems in the real world. Future studies should consider more realistic conditions (e.g., the existence of temperature gradients in the treatment units, the dynamic temperatures of sludge and sludge treatment units over time, varying SRTs, and non-steady-state heat transfer conditions) to better reflect the complex nature of the HT-coupled AD systems.

Second, this work does not include many critical environmental considerations related to the HT-coupled AD processes. When conducting the energy and economic analysis, this work considers only the energy balance, the capture and valorization of carbon dioxide, and the economic aspects of the HT-coupled AD systems. Many critical environmental considerations of the processes are not covered, such as the inactivation of pathogens, antimicrobial resistance genes, and antimicrobial resistant bacteria; the transformation, mobility, and recovery of nutrients; the production of value-added products (e.g., biofuels and precursors of functional materials); the evolution of the speciation and the changes of the toxicity of heavy metals; and the safe disposal or land application of the residual sludge. Future studies should include more critical environmental considerations when analyzing the energy and economic aspects of the HT-coupled AD systems.

Third, this work is based solely on technology and economy, thus lacking regulatory and policy considerations. When analyzing the energy and economic aspects of the HT-coupled AD systems, this work considers only the energy, technological, and economic aspects. However, the energy and economic aspects of the sludge treatment systems in the real world are heavily affected by laws, regulations, subsidies, and policies related to environmental protection and sustainability, renewable energy, greenhouse gas emission control, public health, and waste management. Therefore, future work should incorporate regulatory and policy considerations into the energy and economic assessments of the HT-coupled AD systems.

Fourth, this work lacks a comprehensive sensitivity analysis for the key parameters that affect the energy and economic aspects of the HT-coupled AD systems. For instance, this study assumes that the electricity conversion efficiency for a CHP unit is fixed at 35%. In addition, this work uses the recent wholesale market prices of the surplus heat and electricity in the economic analysis. Because of the lack of a comprehensive sensitivity analysis, it is unclear how the overall energy and economic aspects of the sludge treatment systems would change when the electricity conversion efficiency changes or when the wholesale prices of heat and electricity fluctuate. Sensitivity analysis provides insights into the robustness of the assessments and should be included in future studies.

In addition to the limitations, this work contains sources of error. The multiple assumptions to simplify the energy balance and economic analysis are the major sources of error. For instance, this work assumes that the heat recovery efficiency of all heat exchangers is fixed at 70%. However, in the real world, the heat recovery efficiency of a heat exchanger is likely below or above 70%, and different heat exchangers in the same system likely have different efficiencies. Thus, this assumption introduces errors into the analysis results. In addition, this study assumes that each AB and the heat transfer anywhere in any system are both at a steady state. However, in real sludge treatment systems, ABs and heat transfer are likely at non-steady-state conditions. The difference between the steady-state conditions (assumed in the analysis in this study) and non-steady-state conditions (existing in real sludge treatment systems) also introduces errors into the results. To minimize the errors, future work should make more realistic assumptions, perform dynamic analysis for non-steady-state conditions, incorporate sensitivity and uncertainty analysis, and validate the theoretical analysis results with experimental data.

4. Conclusions

This study for the first time comprehensively analyzes the energy and economic aspects of three HT-coupled AD processes, each incorporating carbon dioxide capture and valorization, for municipal sewage sludge treatment: A pre-stage system (HT→AD), an inter-stage system (1st AD→HT→2nd AD), and a post-stage system (AD↔HT). Because of the large energy burden of HT, conducting HT to enhance the performance of AD is meaningful only when the HT temperature is low or moderate (≤ 130 °C), the raw sludge has a high organic matter content, and the control (AD only) has a low biogas production (i.e., the raw sludge has a high content of complex, especially particulate, organic matter). By contrast, under many conditions, the increase in biogas production during AD due to HT cannot offset the large energy demand of HT, especially when the control has a high TS destruction and/or when the raw sludge has a low organic matter content. This work proposes three strategies to increase the energy and economic output of an HT-coupled AD system: I) Separating the solids and liquid fractions in the raw sludge through centrifugation and applying HT to only the solids fraction, II) Applying HT to only WAS and digesting the blend of hydrothermally treated WAS and untreated PS, and III) Using direct solar energy as a “free,” renewable energy source to conduct HT. Future municipal sewage sludge treatment systems should consider evaluating and implementing the proposed strategies to be more sustainable and to achieve greater energy and economic benefits. Recovering carbon dioxide from the biogas has significant environmental and economic benefits, which should be explored in future experimental and modeling work to better solve real-life problems. Among the three HT-coupled AD systems, the post-stage/recycle system is more beneficial from an economic viewpoint and should be implemented in future HT-coupled AD systems. Conversely, the inter-stage system should be avoided because it is more complex to maintain, requires a larger footprint, and has less significant economic benefits. The major limitations and sources of error of this work are: I) Its assumptions do not fully reflect the complexity of sludge treatment systems in the real world; II) It does not include many critical environmental considerations; III) It is based solely on technology, energy, and economics, thus lacking regulatory and policy considerations; and IV) A comprehensive sensitivity analysis is not conducted. To address these limitations and sources of error, future work should consider more realistic (e.g., dynamic) conditions; include more environmental, regulatory, and policy considerations; perform sensitivity analysis; and validate the theoretical analysis results with experimental data.

Declaration of competing interest

The authors declare that they have no known competing financial interests or personal relationships that could have appeared to influence the work reported in this paper.

Data availability

Data will be made available on request.

Acknowledgment

This work was supported by the National Science Foundation of the United States (award number 1739884) and the Nathan Deutsch Faculty Development Fund from Arkansas State University (Jonesboro,

Arkansas, U.S.A.).

Declaration of Generative Artificial Intelligence and Artificial-Intelligence-Assisted Technologies in the Writing Process

During the preparation of this work, the authors used ChatGPT 3.5 (chat.openai.com) to: I) better define the purposes and scope of this study; II) help find the limitations and potential sources of error of this work; III) enhance the novelty statement; and IV) increase the readability, concision, consistency, and correctness of some sentences. After using this tool, the authors reviewed, edited, revised, and updated the contents as needed and took full responsibility for the contents of the publication.

References

[1] Devos P, Filali A, Grau P, Gillot S. Sidestream characteristics in water resource recovery facilities: a critical review. Water Res 2023;232:119620.
[2] Liu X, Zhu F, Zhang R, Zhao L, Qi J. Recent progress on biodiesel production from municipal sewage sludge. Renew Sustain Energy Rev 2021;135:110260.
[3] Grady Jr CPL, Daigger GT, Love NG, Filipe CDM. Biological Wastewater Treatment. Third ed. Boca Raton, Florida, U.S.A.: Taylor & Francis Group (CRC Press); 2011.
[4] Jiang Y, Gao F, Zhang N, Li J, Xu M, Jiang Y. Dehydration performance of municipal sludge and its dewatering conditioning methods: a review. Ind Eng Chem Res 2023;62(29):11337–57.
[5] Hoang SA, et al. Treatment processes to eliminate potential environmental hazards and restore agronomic value of sewage sludge: a review. Environ Pollut 2022;293:118564.
[6] Di Giacomo G, Romano P. Evolution and prospects in managing sewage sludge resulting from municipal wastewater purification. Energies 2022;15(15):5633.
[7] Hu M, et al. A review on turning sewage sludge to value-added energy and materials via thermochemical conversion towards carbon neutrality. J Clean Prod 2022;379(Part 1):134657.
[8] Capodaglio AG. Biorefinery of sewage sludge: overview of possible value-added products and applicable process technologies. Water 2023;15(6):1195.
[9] Arias A, Feijoo G, Moreira MT. What is the best scale for implementing anaerobic digestion according to environmental and economic indicators? J Water Proc Eng 2020;35:101235.
[10] Chozhavendhan S, et al. Current and prognostic overview on the strategic exploitation of anaerobic digestion and digestate: a review. Environ Res 2022;216 (Part 2):114526.
[11] Khawer MUB, et al. Anaerobic digestion of sewage sludge for biogas & biohydrogen production: state-of-the-art trends and prospects. Fuel 2022;329:125416.
[12] Rittmann BE, McCarty PL. Environmental Biotechnology: Principles and Applications. Second ed. New York, New York, U.S.A.: McGraw-Hill; 2020.
[13] He ZW, et al. Recent advances and perspectives in roles of humic acid in anaerobic digestion of waste activated sludge. Chem Eng J 2023;466:143081.
[14] Hosseini Koupaie E, et al. Performance evaluation and microbial community analysis of mesophilic and thermophilic sludge fermentation processes coupled with thermal hydrolysis. Renew Sustain Energy Rev 2021;141:110832.
[15] Pilli S, Yan S, Tyagi RD, Surampalli RY. Thermal pretreatment of sewage sludge to enhance anaerobic digestion: a review. Crit Rev Environ Sci Technol 2015;45(6):669–702.
[16] Xiao K, Abbt-Braun G, Horn H. Changes in the characteristics of dissolved organic matter during sludge treatment: a critical review. Water Res 2020;187:116441.
[17] Long S, et al. Multiple roles of humic substances in anaerobic digestion systems: a review. J Clean Prod 2023;418:138066.
[18] Wang J, et al. Unblocking the rate-limiting step of the municipal sludge anaerobic digestion. Water Environ Res 2022;94(10):e10793.
[19] Liu X, Chen Y, Wang H, Yuan S, Dai X. Obtain high quality hydrochar from waste activated sludge with low nitrogen content using acids and alkali pretreatment by enhancing hydrolysis and catalyzation. J Anal Appl Pyrol 2024;177:106315.
[20] Eskicioglu C, Kennedy KJ, Droste RL. Characterization of soluble organic matter of waste activated sludge before and after thermal pretreatment. Water Res 2006;40(20):3725–36.
[21] Nguyen VK, et al. Review on pretreatment techniques to improve anaerobic digestion of sewage sludge. Fuel 2021;285:119105.
[22] Langenhoff AA, Intrachandra N, Stuckey DC. Treatment of dilute soluble and colloidal wastewater using an anaerobic baffled reactor: influence of hydraulic retention time. Water Res 2000;34(4):1307–17.
[23] Gahlot P, et al. Principles and potential of thermal hydrolysis of sewage sludge to enhance anaerobic digestion. Environ Res 2022;214(Part 2):113856.
[24] Guo Y, Askari N, Smets I, Appels L. A review on co-metabolic degradation of organic micropollutants during anaerobic digestion: linkages between functional groups and digestion stages. Water Res 2024;256:121598.
[25] Mitraka GC, Kontogiannopoulos KN, Batsioula M, Banias GF, Zouboulis AI, Kougias PG. A comprehensive review on pretreatment methods for enhanced biogas production from sewage sludge. Energies 2022;15(18):6536.
[26] Kakar FL, Tadesse F, Elbeshbishy E. Comprehensive review of hydrothermal pretreatment parameters affecting fermentation and anaerobic digestion of municipal sludge. Processes 2022;10(12):2518.
[27] Zou J, Liu X, Xu S, Chen M, Yu Q, Xie J. Combined hydrothermal pretreatment of agricultural and forestry wastes to enhance anaerobic digestion for methane production. Chem Eng J 2024;486:150313.
[28] Aragón-Briceño C, Ross A, Camargo-Valero M. Strategies for the revalorization of sewage sludge in a waste water treatment plant through the integration of hydrothermal processing. Waste Biomass Valori 2023;14:105–26.
[29] Chen Q, et al. The function of "Cambi® thermal hydrolysis + anaerobic digestion" on heavy metal behavior and risks in a full-scale sludge treatment plant based on four seasons investigation. J Hazard Mater 2023;445:130579.
[30] Gao Y, Remón J, Matharu AS. Microwave-assisted hydrothermal treatments for biomass valorisation: a critical review. Green Chem 2021;23(10):3502–25.
[31] Zhang B, Biswal BK, Zhang J, Balasubramanian R. Hydrothermal treatment of biomass feedstocks for sustainable production of chemicals, fuels, and materials: progress and perspectives. Chem Rev 2023;123(11):7193–294.
[32] Kruse A, Dahmen N. Hydrothermal biomass conversion: quo vadis? J Supercrit Fluids 2018;134:114–23.
[33] Zhang W, et al. Machine learning for hydrothermal treatment of biomass: a review. Bioresour Technol 2023;370:128547.
[34] Djandja OS, Yin LX, Wang ZC, Duan PG. From wastewater treatment to resources recovery through hydrothermal treatments of municipal sewage sludge: a critical review. Process Saf Environ Protect 2021;151:101–27.
[35] Uthirakrishnan U, et al. Current advances and future outlook on pretreatment techniques to enhance biosolids disintegration and anaerobic digestion: a critical review. Chemosphere 2022;288:132553.
[36] Ortega-Martinez E, Sapkaite I, Fdz-Polanco F, Donoso-Bravo A. From pre-treatment toward inter-treatment. Getting some clues from sewage sludge biomethanation. Bioresour Technol 2016;212:227–35.
[37] Aragón-Briceño C, Ross A, Camargo-Valero M. Evaluation and comparison of product yields and bio-methane potential in sewage digestate following hydrothermal treatment. Appl Energy 2017;208:1357–69.
[38] Zhang C, Liu X, Wang Q, Tang Y, Pavlostathis SG. Comparative assessment of pre- and inter-stage hydrothermal treatment of municipal sludge for increased methane production. Water Environ Res 2021;93(7):1126–37.
[39] Yuan T, Cheng Y, Zhang Z, Lei Z, Shimizu K. Comparative study on hydrothermal treatment as pre-and post-treatment of anaerobic digestion of primary sludge: focus on energy balance, resources transformation and sludge dewaterability. Appl Energy 2019;239:171–80.
[40] Chen P, et al. Optimal deployment of thermal hydrolysis and anaerobic digestion to maximize net energy output based on sewage sludge characteristics. Water Res 2023;247:120767.
[41] Takashima M. Examination on process configurations incorporating thermal treatment for anaerobic digestion of sewage sludge. J Environ Eng 2008;134(7):543–9.
[42] Nuchdang S, Frigon JC, Roy C, Pilon G, Phalakornkule C, Guiot S. Hydrothermal post-treatment of digestate to maximize the methane yield from the anaerobic digestion of microalgae. Waste Manag 2018;71:683–8.
[43] Yang D, Hu C, Dai L, Liu Z, Dong B, Dai X. Post-thermal hydrolysis and centrate recirculation for enhancing anaerobic digestion of sewage sludge. Waste Manag 2019;92:39–48.
[44] Campo G, Cerutti A, Zanetti M, Scibilia G, Lorenzi E, Ruffino B. Enhancement of waste activated sludge (WAS) anaerobic digestion by means of pre-and intermediate treatments. Technical and economic analysis at a full-scale WWTP. J Environ Manag 2018;216:372–82.
[45] Passos F, Ferrer I. Influence of hydrothermal pretreatment on microalgal biomass anaerobic digestion and bioenergy production. Water Res 2015;68:364–73.
[46] Wang X, Jiang C, Wang H, Xu S, Zhuang X. Strategies for energy conversion from sludge to methane through pretreatment coupled anaerobic digestion: potential energy loss or gain. J Environ Manag 2023;330:117033.
[47] Wang M, Liu K, Wang J, Li Y, Peng H, Ding L. Comparison and improvement of energy balance establishment methods for heat pretreatment prior to anaerobic digestion. Fuel 2024;368:131579.
[48] Liu X, Wang Q, Tang Y, Pavlostathis SG. Hydrothermal pretreatment of sewage sludge for enhanced anaerobic digestion: resource transformation and energy balance. Chem Eng J 2021;410:127430.
[49] Ipiales R, de La Rubia M, Diaz E, Mohedano A, Rodriguez JJ. Integration of hydrothermal carbonization and anaerobic digestion for energy recovery of biomass waste: an overview. Energy Fuels 2021;35(21):17032–50.
[50] Bohutskyi P, Phan D, Spierling RE, Lundquist TJ. Hydrothermal but not mechanical pretreatment of wastewater algae enhanced anaerobic digestion energy balance due to improved biomass disintegration and methane production kinetics. Energies 2023;16(20):7146.
[51] Balasundaram G, et al. Energy feasibility and life cycle assessment of sludge pretreatment methods for advanced anaerobic digestion. Bioresour Technol 2022;357:127345.
[52] Liu X, Wang Q, Tang Y, Pavlostathis SG. A comparative study on biogas production, energy balance, and nutrients conversion with inter-stage hydrothermal treatment of sewage sludge. Appl Energy 2021;288:116669.
[53] Panchenko V, Kovalev A, Kovalev D, Litty YV. Review of modern methods and technologies for using of solar energy in the operation of anaerobic digestion systems. Int J Hydrogen Energy 2023;48(53):20264–78.
[54] Huang W, Zhao Z, Yuan T, Huang W, Lei Z, Zhang Z. Low-temperature hydrothermal pretreatment followed by dry anaerobic digestion: a sustainable strategy for manure waste management regarding energy recovery and nutrients availability. Waste Manag 2017;70:255–62.
[55] Passos F, Ferrer I. Microalgae conversion to biogas: thermal pretreatment contribution on net energy production. Environ Sci Technol 2014;48(12):7171–8.

[56] Esposito E, Dellamuzia L, Moretti U, Fuoco A, Giorno L, Jansen JC. Simultaneous production of biomethane and food grade CO_2 from biogas: an industrial case study. Energy Environ Sci 2019;12(1):281–9.

[57] Farghali M, Osman AI, Umetsu K, Rooney DW. Integration of biogas systems into a carbon zero and hydrogen economy: a review. Environ Chem Lett 2022;20(5): 2853–927.

[58] Ziemba C, Peccia J. Net energy production associated with pathogen inactivation during mesophilic and thermophilic anaerobic digestion of sewage sludge. Water Res 2011;45(16):4758–68.

[59] Wang S, Ruan Y, Zhou W, Li Z, Wu J, Liu D. Net energy analysis of small-scale biogas self-supply anaerobic digestion system operated at psychrophilic to thermophilic conditions. J Clean Prod 2018;174:226–36.

[60] Gebremedhin K, Wu B, Gooch C, Wright P, Inglis S. Heat transfer model for plug-flow anaerobic digesters. Transactions of the ASAE 2005;48(2):777–85.

[61] Kwon YJ, Lee DK. Thermal comfort and longwave radiation over time in urban residential complexes. Sustainability 2019;11(8):2251.

[62] Kumar S, Lohan SK, Parihar DS. Biomass energy from agriculture: conversion techniques and use. In: Rakshit A, Biswas A, Sarkar D, Datta R, Meena VS, editors. Handbook of Energy Management in Agriculture. Singapore: Springer Nature Singapore Pte Ltd.; 2023. p. 181–99.

[63] Ghangrekar MM. Sludge management. In: Wastewater to Water: Principles, Technologies and Engineering Design. Singapore: Springer Nature Singapore Pte Ltd.; 2022. p. 619–91.

[64] Guo J, Dong R, Clemens J, Wang W. Thermal modelling of the completely stirred anaerobic reactor treating pig manure at low range of mesophilic conditions. J Environ Manag 2013;127:18–22.

[65] Hashimoto AG, Chen YR, Varel VH. Anaerobic Fermentation of Beef Cattle Manure. Solar Energy Research Institute (A Division of Midwest Research Institute). 1981 Golden, Colorado, U.S.A.

[66] Packer J. Commercialisation of fuel cells for combined heat and power (CHP) application. J Power Sources 1992;37(1–2):101–9.

[67] Le Cam A, Southernwood J, Ring D, Clarke D, Creedon R. Impact of demand response on occupants' thermal comfort in a leisure center. Energy Efficiency 2021;14:91.

[68] Chowdhury T. Technical-economical analysis of anaerobic digestion process to produce clean energy. Energy Rep 2021;7:247–53.

[69] Caposciutti G, Baccioli A, Ferrari L, Desideri U. Biogas from anaerobic digestion: power generation or biomethane production? Energies 2020;13(3):743.

[70] Merlin G, Kohler F, Bouvier M, Lissolo T, Boileau H. Importance of heat transfer in an anaerobic digestion plant in a continental climate context. Bioresour Technol 2012;124:59–67.

[71] Jones PD, New M, Parker DE, Martin S, Rigor IG. Surface air temperature and its changes over the past 150 years. Rev Geophys 1999;37(2):173–99.

[72] Oliva A, Tan L, Papirio S, Esposito G, Lens P. Use of N-Methylmorpholine N-oxide (NMMO) pretreatment to enhance the bioconversion of lignocellulosic residues to methane. Biomass Convers and Bior 2024;14(10):11113–30.

[73] Zheng D, Hunt Jr ER, Running SW. A daily soil temperature model based on air temperature and precipitation for continental applications. Clim Res 1993;2(3): 183–91.

[74] Gu X, Huang Y, Hu Y, Huang W, Zhang M. Impact of nitrite on partial nitrification in aerobic sewage treatment reactors under mainstream conditions. J Environ Chem Eng 2022;10(5):108414.

[75] Zuo F, Yue W, Gui S, Sui Q, Wei Y. Resilience of anammox application from sidestream to mainstream: a combined system coupling denitrification, partial nitritation and partial denitrification with anammox. Bioresour Technol 2023; 374:128783.

[76] Nabaterega R, Kumar V, Khoei S, Eskicioglu C. A review on two-stage anaerobic digestion options for optimizing municipal wastewater sludge treatment process. J Environ Chem Eng 2021;9(4):105502.

[77] Nges IA, Liu J. Effects of solid retention time on anaerobic digestion of dewatered-sewage sludge in mesophilic and thermophilic conditions. Renew Energy 2010;35 (10):2200–6.

[78] Mehdizadeh SN, Eskicioglu C, Bobowski J, Johnson T. Conductive heating and microwave hydrolysis under identical heating profiles for advanced anaerobic digestion of municipal sludge. Water Res 2013;47(14):5040–51.

[79] Liu J, Zheng J, Zhang J, Yu D, Wei Y. The performance evaluation and kinetics response of advanced anaerobic digestion for sewage sludge under different SRT during semi-continuous operation. Bioresour Technol 2020;308:123239.

[80] Chen Y, Xiao K, Jiang X, Shen N, Zeng RJ, Zhou Y. Long solid retention time (SRT) has minor role in promoting methane production in a 65 °C single-stage anaerobic sludge digester. Bioresour Technol 2018;247:724–9.

[81] Tiwari GN, Shyam Tiwari A. Handbook of Solar Energy: Theory, Analysis and Applications (Energy Systems in Electrical Engineerin). Singapore: Springer Nature (Springer Science+Business Media Singapore Pte Ltd.); 2016.

[82] Tiwari GN, Sahota L. Advanced Solar-Distillation Systems: Basic Principles, Thermal Modeling, and Its Application (Green Energy and Technology). Singapore: Springer Nature (Springer Nature Singapore Pte Ltd.); 2017.

[83] Li C, et al. Synergistic treatment of sewage sludge and food waste digestate residues for efficient energy recovery and biochar preparation by hydrothermal pretreatment, anaerobic digestion, and pyrolysis. Appl Energy 2024;364:123203.

[84] Ngo PL, Udugama IA, Gernaey KV, Young BR, Baroutian S. Mechanisms, status, and challenges of thermal hydrolysis and advanced thermal hydrolysis processes in sewage sludge treatment. Chemosphere 2021;281:130890.

[85] Mikusińska J, Kuźnia M, Czerwińska K, Wilk M. Hydrothermal carbonization of digestate produced in the biogas production process. Energies 2023;16(14):5458.

[86] Mutegoa E, Sahini MG. Approaches to mitigation of hydrogen sulfide during anaerobic digestion process–a review. Heliyon 2023;9(9):e19768.

[87] Li Y, et al. Composition and toxicity of biogas produced from different feedstocks in California. Environ Sci Technol 2019;53(19):11569–79.

[88] Shi Y, Xu J. A multi-objective approach to kitchen waste and excess sludge co-digestion for biomethane production with anaerobic digestion. Energy 2023;262 (Part A):125243.

[89] Kabouris JC, et al. Methane recovery from the anaerobic codigestion of municipal sludge and FOG. Bioresour Technol 2009;100(15):3701–5.

[90] Ye J, Mu Y, Cheng X, Sun D. Treatment of fresh leachate with high-strength organics and calcium from municipal solid waste incineration plant using UASB reactor. Bioresour Technol 2011;102(9):5498–503.

[91] Chen R, et al. Life-cycle assessment of two sewage sludge-to-energy systems based on different sewage sludge characteristics: energy balance and greenhouse gas-emission footprint analysis. J Environ Sci 2022;111:380–91.

[92] Liu C, Li H, Zhang Y, Liu C. Improve biogas production from low-organic-content sludge through high-solids anaerobic co-digestion with food waste. Bioresour Technol 2016;219:252–60.

[93] Li H, Jin C, Zhang Z, O'Hara I, Mundree S. Environmental and economic life cycle assessment of energy recovery from sewage sludge through different anaerobic digestion pathways. Energy 2017;126:649–57.

[94] Montusiewicz A, Lebiocka M. Co-digestion of intermediate landfill leachate and sewage sludge as a method of leachate utilization. Bioresour Technol 2011;102 (3):2563–71.

[95] The United States Environmental Protection Agency. Process Design Manual for Sludge Treatment and Disposal. 1979. Washington, D.C., U.S.A., EPA 625/1-79-011.

[96] The Engineering ToolBox. "Surface Emissivity Coefficients: The Radiation Heat Transfer Emissivity Coefficients for Some Common Materials Like Aluminum, Brass, Glass and Many More." engineeringtoolbox.com/emissivity-coefficients-d_447.html (accessed 2023).

[97] The Engineering ToolBox. "Absorbed Solar Radiation: Solar Radiation Absorbed by Various Materials." engineeringtoolbox.com/solar-radiation-absorbed-materials-d_1568.html (accessed 2023).

[98] Metcalf & Eddy, Inc., Burton F, Stensel H, Tchobanoglous G, Tsuchihashi R. Wastewater Engineering: Treatment and Resource Recovery. Fifth ed. New York, New York, U.S.A: McGraw-Hill; 2014.

[99] Tang WZ, Sillanpää M. Sustainable Environmental Engineering. Hoboken, New Jersey, U.S.A.: John Wiley & Sons, Inc.; 2018.

[100] Li L, et al. Photothermal Ti_2O_3/polyurethane/polyacrylamide foam with high solar-evaporation efficiency. Desalination 2023;567:117001.

[101] Haffiez N, et al. A critical review of process parameters influencing the fate of antibiotic resistance genes in the anaerobic digestion of organic waste. Bioresour Technol 2022;354:127189.

[102] Ashare E, Wise DL, Wentworth RL. Fuel Gas Production from Animal Residue-Engineering Report (Dynatech Report No. 1551). Cambridge, Massachusetts, U.S. A.: Dynatech R/D Company; 1977.

[103] Wiegleb G. Physical properties of gases. In: In: Gas Measurement Technology in Theory and Practice: Measuring Instruments, Sensors, Applications. Wiesbaden, Germany: Springer Nature (Springer Fachmedien Wiesbaden GmbH); 2023. p. 7–125.

[104] The Engineering ToolBox. "Methane Gas - Specific Heat vs. Temperature: Specific Heat of Methane Gas - CH_4 - at Temperatures Ranging 200 - 1100 K." engineeringtoolbox.com/methane-d_980.html (accessed 2023).

[105] Kakar FL, Liss SN, Elbeshbishy E. Impact of solid content on hydrothermal pretreatment of municipal sludge prior to fermentation and anaerobic digestion. Chemosphere 2022;308(Part 3):136363.

[106] Wang C, et al. Acclimatizing waste activated sludge in a thermophilic anaerobic fixed-bed biofilm reactor to maximize biogas production for food waste treatment at high organic loading rates. Water Res 2023;242:120299.

[107] Ahnert M, Schalk T, Brückner H, Effenberger J, Kuehn V, Krebs P. Organic matter parameters in WWTP–a critical review and recommendations for application in activated sludge modelling. Water Sci Technol 2021;84(9):2093–112.

[108] Igoni AH, Ayotamuno M, Eze C, Ogaji S, Probert S. Designs of anaerobic digesters for producing biogas from municipal solid-waste. Appl Energy 2008;85(6):430–8.

[109] The Engineering ToolBox. "Carbon Dioxide Gas - Specific Heat vs. Temperature: Specific Heat of Carbon Dioxide Gas - CO_2 - Temperatures Ranging 175 - 6000 K." engineeringtoolbox.com/carbon-dioxide-d_974.html (accessed 2023).

[110] Sawyer CN, McCarty PL, Parkin GF. Chemistry for Environmental Engineering and Science. Fifth ed. New York, New York, U.S.A.: The McGraw-Hill Companies, Inc. (McGraw-Hill Higher Education); 2003.

[111] Lowe PR, Ficke JM. The Computation of Saturation Vapor Pressure. Monterey, California, U.S.A.: Environmental Prediction Research Facility (Navy);; 1974.

[112] Murray FW. On the computation of saturation vapor pressure. J Appl Meteorol 1967;6:203–4.

[113] Goff JA, Gratch S. Low-pressure properties of water - from 160 to 212 °F. Trans Am Heat Vent Eng (52nd annual meeting of the American Society of Heating and Ventilating Engineers, New York U.S.A.) 1946:95–122.

[114] The Engineering ToolBox. "Water Vapor - Specific Heat vs. Temperature: Specific Heat of Water Vapor - H_2O - at Temperatures Ranging 175 - 6000 K." engineeringtoolbox.com/water-vapor-d_979.html (accessed 2023).

[115] The Engineering ToolBox. "Water - Heat of Vaporization vs. Temperature: Online Calculator, Figures and Tables Showing Heat of Vaporization of Water, at Temperatures from 0 - 370 °C (32 - 700 °F) - SI and Imperial Units." engineeringtoolbox.com/water-properties-d_1573.html (accessed 2023).

[116] Lu J, Gavala HN, Skiadas IV, Mladenovska Z, Ahring BK. Improving anaerobic sewage sludge digestion by implementation of a hyper-thermophilic prehydrolysis step. J Environ Manag 2008;88(4):881–9.

[117] Çengel YA, Cimbala JM, Turner RH. Fundamentals of Thermal-Fluid Sciences. Fifth ed. New York, New York, U.S.A.: McGraw-Hill Education; 2017.

[118] Yu Y, Tang Y, Chou J, Yang L. A novel adaptive approach for improvement in the estimation of hourly diffuse solar radiation: a case study of China. Energy Convers Manag 2023;293:117455.

[119] Bai RL, Jin L, Sun SR, Cheng Y, Wei Y. Quantification of greenhouse gas emission from wastewater treatment plants. Greenhouse Gas Sci Technol 2022;12(5):587–601.

[120] von Stockar U, Liu JS. Does microbial life always feed on negative entropy? Thermodynamic analysis of microbial growth. Biochim Biophys Acta 1999;1412(3):191–211.

[121] Singh V, Phuleria HC, Chandel MK. Estimation of energy recovery potential of sewage sludge in India: waste to watt approach. J Clean Prod 2020;276:122538.

[122] Schaum C, Lensch D, Cornel P. Evaluation of the energetic potential of sewage sludge by characterization of its organic composition. Water Sci Technol 2016;73(12):3072–9.

[123] Zanoni AE, Mueller DL. Calorific value of wastewater plant sludges. J Environ Eng Div 1982;108(1):187–95.

[124] Shizas I, Bagley DM. Experimental determination of energy content of unknown organics in municipal wastewater streams. J Energy Eng 2004;130(2):45–53.

[125] Higgins MJ, et al. Pretreatment of a primary and secondary sludge blend at different thermal hydrolysis temperatures: impacts on anaerobic digestion, dewatering and filtrate characteristics. Water Res 2017;122:557–69.

[126] Segeler CG. Gas Engineers Handbook: Fuel Gas Engineering Practices. New York, U.S.A.: Industrial Press, Inc.; 1965.

[127] Baldwin A, Lovell-Smith J. The emissivity of stainless steel in dairy plant thermal design. J Food Eng 1992;17(4):281–9.

[128] Graves R, Kollie T, McElroy D, Gilchrist K. The thermal conductivity of AISI 304L stainless steel. Int J Thermophys 1991;12(2):409–15.

[129] Assael M, Gialou K. Measurement of the thermal conductivity of stainless steel AISI 304L up to 550 K. Int J Thermophys 2003;24(4):1145–53.

[130] Yener T, Yener ŞÇ, Mutlu R. Convection coefficient estimation of still air using an infrared thermometer and curve-fitting. J of Eng Tech and App Sci 2019;4(2):95–103.

[131] Kreith F, Manglik Bohn MS RM. Principles of Heat Transfer. Seventh ed. Stamford, Connecticut, U.S.A.: Cengage Learning, Inc.; 2011.

[132] Incropera FP, DeWitt DP, Bergman TL, Lavine AS. Fundamentals of Heat and Mass Transfer. Sixth ed. Hoboken, New Jersey, U.S.A: John Wiley & Sons, Inc.; 2007.

[133] Kavitha S, Banu JR, Priya AA, Uan DK, Yeom IT. Liquefaction of food waste and its impacts on anaerobic biodegradability, energy ratio and economic feasibility. Appl Energy 2017;208:228–38.

[134] Zupančič GD, Roš M. Heat and energy requirements in thermophilic anaerobic sludge digestion. Renew Energy 2003;28(14):2255–67.

[135] Baumgartner T, Jahn L, Parravicini V, Svardal K, Krampe J. Efficiency of sidestream nitritation for modern two-Stage activated sludge plants. Int J Environ Res Publ Health 2022;19(19):12871.

[136] Yoshida Y, et al. Comprehensive comparison of efficiency and CO_2 emissions between biomass energy conversion technologies—position of supercritical water gasification in biomass technologies. Biomass Bioenergy 2003;25(3):257–72.

[137] Maga D. Life cycle assessment of biomethane produced from microalgae grown in municipal waste water. Biomass Convers and Bior 2017;7(1):1–10.

[138] Arsalis A, Kær SK, Nielsen MP. Modeling and optimization of a heat-pump-assisted high temperature proton exchange membrane fuel cell micro-combined-heat-and-power system for residential applications. Appl Energy 2015;147:569–81.

[139] Granovskii M, Dincer I, Rosen MA. Performance comparison of two combined SOFC–gas turbine systems. J Power Sources 2007;165(1):307–14.

[140] Wu H, Jouhara H, Tassou S, Karayiannis T. Modelling of energy flows in potato crisp frying processes. Appl Energy 2012;89(1):81–8.

[141] Cullen JM, Allwood JM. Theoretical efficiency limits for energy conversion devices. Energy 2010;35(5):2059–69.

[142] The United States Energy Information Administration. "U.S. Henry Hub Natural Gas Price Expected to Increase from Recent Lows." www.eia.gov/todayinenergy/detail.php?id=56501 (accessed 2023).

[143] The United States Energy Information Administration. "Wholesale Electricity and Natural Gas Market Data." www.eia.gov/electricity/wholesale/#history (accessed 2023).

[144] Demirel Y. Energy conservation. In: Energy: Production, Conversion, Storage, Conservation, and Coupling (Green Energy and Technology). Second ed. Cham, Switzerland: Springer Nature (Springer International Publishing AG Switzerland); 2016. p. 363–418.

[145] Kaya D, Çanka Kılıç F, Öztürk HH. Energy efficiency in pumps. In: Energy Management and Energy Efficiency in Industry: Practical Examples (Green Energy and Technology). Cham, Switzerland: Springer Nature Switzerland AG; 2021. p. 329–74.

[146] Shankar Arun, Kalaiselvan Vishnu, Umashankar S, Paramasivam S, Hanigovszki N. A comprehensive review on energy efficiency enhancement initiatives in centrifugal pumping system. Appl Energy 2016;181:495–513.

[147] Stoffel B. Assessing the Energy Efficiency of Pumps and Pump Units: Background and Methodology. Amsterdam, Netherlands: Elsevier Ltd.; 2015.

[148] The United States Energy Information Administration. "How Much Electricity is Lost in Electricity Transmission and Distribution in the United States?" www.eia.gov/tools/faqs/faq.php?id=105&t=3 (accessed 2023).

[149] Smith TB. Electricity theft: a comparative analysis. Energy Pol 2004;32(18):2067–76.

[150] Liu K, Wang K, Wang S, Wu Q, Hao J. Tracking carbon flows from coal mines to electricity users in China using an ensemble model. Environ Sci Technol 2023;57(33):12242–50.

[151] Makaruk A, Miltner M, Harasek M. Membrane biogas upgrading processes for the production of natural gas substitute. Separ Purif Technol 2010;74(1):83–92.

[152] Li S, Ding J, Zhang X, Cheng D, Hu X, Li X. A feasible energy-saving analysis of a new system for CO_2 cryogenic capture. Int J Low Carbon Technol 2016;11(2):235–9.

[153] Jackson S, Brodal E. A comparison of the energy consumption for CO_2 compression process alternatives. 8th International Conference on Environment Science and Engineering (ICESE 2018; Barcelona, Spain) 2018:012031. IOP Conference Series: Earth and Environmental Science 167.

[154] Lee U, Yang S, Jeong YS, Lim Y, Lee CS, Han C. Carbon dioxide liquefaction process for ship transportation. Ind Eng Chem Res 2012;51(46):15122–31.

[155] Øi LE, Eldrup N, Adhikari U, Bentsen MH, Badalge JL, Yang S. Simulation and cost comparison of CO_2 liquefaction. Energy Proc 2016;86:500–10.

[156] The United States Energy Information Administration. "Electric Power Monthly: Table 5.3. Average Price of Electricity to Ultimate Customers." www.eia.gov/electricity/monthly/epm_table_grapher.php?t=epmt_5_03 (accessed 2023).

[157] ChemAnalyst. "Liquid Carbon Dioxide Price Trend and Forecast." www.chemanalyst.com/Pricing-data/liquid-carbon-dioxide-1090 (accessed 2023).

[158] Made-in-China. "Food Grade Carbon Dioxide." www.made-in-china.com/products-search/hot-china-products/Food_Grade_Carbon_Dioxide.html (accessed 2023).

[159] Al-Ghussain L. Global warming: review on driving forces and mitigation. Environ Prog Sustain Energy 2019;38(1):13–21.

[160] Verma A, Arora MS, Omar A, Chauhan K. Optimal control of global warming by carbon dioxide mitigation through awareness programmes. Int J Environ Res 2024;18(4):55.

[161] The United States Department of Energy (Industrial Efficiency & Decarbonization Office). "U.S. Department of Energy Announces $121 Million to Reduce Emissions across America's Industrial Sector." www.energy.gov/eere/iedo/articles/us-department-energy-announces-121-million-reduce-emissions-across-americas?utm_medium=email&utm_source=govdelivery (accessed 2023).

[162] Atelge M, et al. A critical review of pretreatment technologies to enhance anaerobic digestion and energy recovery. Fuel 2020;270:117494.

[163] Chen R, Dai X, Dong B. Two birds with one stone: the multiple roles of hydrothermal treatment in dewatering municipal sludge and producing value-added products. Sci Total Environ 2023;896:165072.

[164] Alves O, Calado L, Panizio RM, Gonçalves M, Monteiro E, Brito P. Techno-economic study for a gasification plant processing residues of sewage sludge and solid recovered fuels. Waste Manag 2021;131:148–62.

[165] Lucian M, et al. Hydrothermal carbonization coupled with anaerobic digestion for the valorization of the organic fraction of municipal solid waste. Bioresour Technol 2020;314:123734.

[166] Chu C, Lee D, Chang C. Energy demand in sludge dewatering. Water Res 2005;39(9):1858–68.

[167] Najjar YS, Abu-Shamleh A. Harvesting of microalgae by centrifugation for biodiesel production: a review. Algal Res 2020;51:102046.

[168] Suh Y-J, Rousseaux P. An LCA of alternative wastewater sludge treatment scenarios. Resour Conserv Recycl 2002;35(3):191–200.

[169] Turovskiy IS, Mathai PK. Wastewater Sludge Processing. Hoboken, New Jersey, U.S.A.: John Wiley & Sons, Inc. (Wiley-Interscience); 2006.

[170] Gonzalez A, Hendriks A, Van Lier J, De Kreuk M. Pre-treatments to enhance the biodegradability of waste activated sludge: elucidating the rate limiting step. Biotechnol Adv 2018;36(5):1434–69.

[171] Sakaveli F, Petala M, Tsiridis V, Darakas E. Enhanced mesophilic anaerobic digestion of primary sewage sludge. Water 2021;13(3):348.

[172] Sabiha M, Saidur R, Mekhilef S, Mahian O. Progress and latest developments of evacuated tube solar collectors. Renew Sustain Energy Rev 2015;51:1038–54.

[173] Hayek M, Assaf J, Lteif W. Experimental investigation of the performance of evacuated-tube solar collectors under eastern Mediterranean climatic conditions. Energy Proc 2011;6:618–26.

[174] Mevada D, et al. Applications of evacuated tubes collector to harness the solar energy: a review. Int J Ambient Energy 2022;43(1):344–61.